The Journal of Physiology

Intrinsic motoneuron properties in typical human development

Ghazaleh Mohammadalinejad[1,2,3], Babak Afsharipour[1,2,3], Alex Yacyshyn[1,2], Jennifer Duchcherer[1,2], Jack Bashuk[1,2], Erin Bennett[1,2], Gregory E. P. Pearcey[4], Francesco Negro[5], Katharina A. Quinlan[6], David J. Bennett[2,7] and Monica A. Gorassini[1,2,3]

[1]*Department of Medicine, Faculty of Medicine and Dentistry, University of Alberta, Edmonton, AB, Canada*
[2]*Neuroscience and Mental Health Institute, University of Alberta, Edmonton, AB, Canada*
[3]*Women and Children's Health Research Institute, University of Alberta, Edmonton, AB, Canada*
[4]*School of Human Kinetics and Recreation, Memorial University of Newfoundland, St John's Canada and Physical Therapy & Human Movement Sciences, Northwestern University, Chicago, IL, USA*
[5]*Clinical and Experimental Sciences, Universita degli Studi di Brescia, Brescia, Italia*
[6]*George and Anne Ryan Institute for Neuroscience, Biomedical and Pharmaceutical Sciences, College of Pharmacy, University of Rhode Island, Kingston, RI, USA*
[7]*Faculty of Rehabilitation Medicine, University of Alberta, Edmonton, AB, Canada*

Handling Editors: Richard Carson & Madeleine Lowery

The peer review history is available in the Supporting Information section of this article (https://doi.org/10.1113/JP285756#support-information-section).

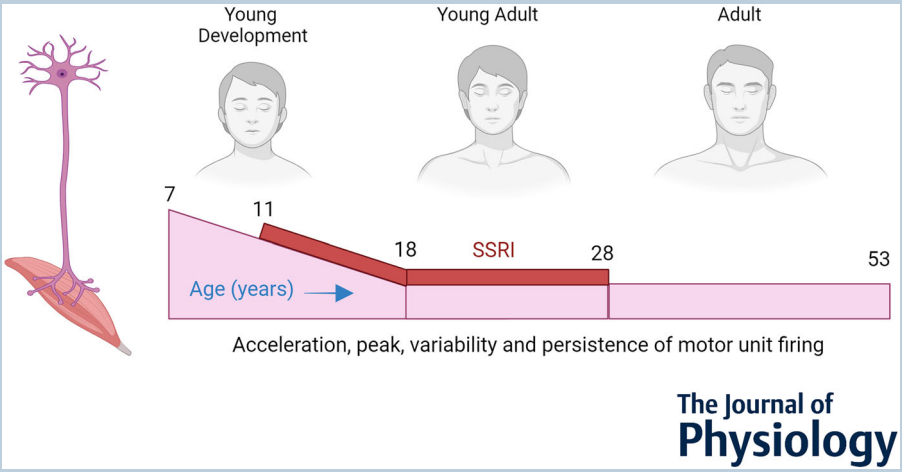

Abstract Motoneuron properties and their firing patterns undergo significant changes throughout development and in response to neuromodulators such as serotonin. Here, we examined the age-related development of self-sustained firing and general excitability of tibialis anterior motoneurons in a young development (7–17 years), young adult (18–28 years) and adult (32–53 years) group, as well as in a separate group of participants taking selective serotonin reuptake

Ghazaleh Mohammdalinejad earned her Master's degree in Neuroscience from the University of Alberta in 2023, having previously completed a Bachelor's degree in Electrical Engineering from Sharif University of Technology in 2020. Throughout her Master's project, Ghazaleh explored the firing behaviour of human motoneurons via single motor unit recordings, specifically investigating how intrinsic motoneuron properties change during development from child to adulthood. Such data will be used to examine dysfunction in motoneuron behaviour following early brain injury. In her current role as a Research Analyst at the Centre for Addiction and Mental Health, she analyses functional magnetic resonance imaging data, providing valuable insights to advance the field of mental health and addiction research.

DOI: 10.1113/JP285756

inhibitors (SSRIs, aged 11–28 years). Self-sustained firing, as measured by ΔF, was larger in the young development (~5.8 Hz, $n = 20$) compared to the young adult (~4.9 Hz, $n = 13$) and adult (~4.8 Hz, $n = 8$) groups, consistent with a developmental decrease in self-sustained firing mediated by persistent inward currents (PIC). ΔF was also larger in participants taking SSRIs (~6.5 Hz, $n = 9$) compared to their age-matched controls (~5.3 Hz, $n = 26$), consistent with increased levels of spinal serotonin facilitating the motoneuron PIC. Participants in the young development and SSRI groups also had higher firing rates and a steeper acceleration in initial firing rates (secondary ranges), consistent with the PIC producing a steeper acceleration in membrane depolarization at the onset of motoneuron firing. In summary, both the young development and SSRI groups exhibited increased intrinsic motoneuron excitability compared to the adults, which, in the young development group, was also associated with a larger unsteadiness in the dorsiflexion torque profiles. We propose several intrinsic and extrinsic factors that affect both motoneuron PICs and cell discharge which vary during development, with a time course similar to the changes in motoneuron firing behaviour observed in the present study.

(Received 27 October 2023; accepted after revision 6 March 2024; first published online 30 March 2024)
Corresponding author M. A. Gorassini: 5 005-A Katz Group Building, University of Alberta, Edmonton, AB, T6G 2E1, Canada. Email: monica.gorassini@ualberta.ca

Abstract figure legend The firing behaviour of multiple, single motor units from the tibialis anterior muscle was decomposed from high-density surface EMG to examine changes in motoneuron excitability across different phases of development from child to adulthood in 50 participants aged 7–53 years. Compared to adults (≥18 years: young adult and adult groups), motor unit discharge of children and adolescents aged 7–17 years (young development group) accelerated faster at the onset of firing, reached higher peak rates and displayed longer self-sustained firing as represented by the amplitude of the pink boxes. Participants aged 11–28 years (red bar), taking serotonin reuptake inhibitors (SSRI) that are known to increase motoneuron excitability by facilitating persistent inward currents, had the highest measures of motoneuron excitability. High motoneuron excitability may contribute to some of the force unsteadiness during the execution of skilled ankle movements observed at the younger ages of development.

Key points

- Neurons in the spinal cord that activate muscles in the limbs (motoneurons) undergo increases in excitability shortly after birth to help animals stand and walk.
- We examined whether the excitability of human ankle flexor motoneurons also continues to change from child to adulthood by recording the activity of the muscle fibres they innervate.
- Motoneurons in children and adolescents aged 7–17 years (young development group) had higher signatures of excitability that included faster firing rates and more self-sustained activity compared to adults aged ≥18 years.
- Participants aged 11–28 years of age taking serotonin reuptake inhibitors had the highest measures of motoneuron excitability compared to their age-matched controls.
- The young development group also had more unstable contractions, which might partly be related to the high excitability of the motoneurons.

Introduction

Spinal motoneurons in rodents undergo marked changes in intrinsic electrical properties during the first 3 weeks of postnatal development. These changes help to facilitate motoneuron recruitment and repetitive firing that are needed for sustained motor behaviours such as posture and weight bearing locomotion (Carrascal et al., 2005; Jean-Xavier et al., 2018). One such marked change is the decrease in threshold and increase in amplitude of persistent inward currents (PICs) in the first 3 weeks after birth (Harris-Warrick et al., 2023; Quinlan et al., 2011; Revill et al., 2019; Sharples & Miles, 2021). PICs are mediated by voltage-activated sodium (Na_V) and calcium (Ca_V) channels (Li et al., 2004) and by a calcium-activated sodium conductance (I_{CaN}) (Bos et al., 2021). Because PICs are activated near the recruitment threshold of the motoneuron, they provide an additional depolarization

to amplify synaptic inputs, help secure the recruitment of the motoneuron and accelerate their initial firing rates (Bennett et al., 1998; Bennett, Li Siu et al., 2001; Gorassini et al., 1998; Hounsgaard et al., 1988; Kiehn & Eken, 1997; Lee & Heckman, 2000; Lee et al., 2003; Li et al., 2004). Thus, the initial period of firing rate acceleration during a slowly increasing input, termed secondary range (Bennett et al., 1998; Granit et al., 1966; Kernell, 1965; Li et al., 2004), is partly a reflection of the onset activation of the intrinsic PIC in motoneurons.

Following the secondary range, the PIC further shapes the firing behaviour of motoneurons. After the PIC is fully activated and produces a sustained plateau potential, the firing rate of the motoneuron increases linearly in response to an increasing intracellular current injection, but with a much shallower slope (Bennett et al., 1998; Lee et al., 2003). This lower-gain response, termed the tertiary or saturation range, results partly from an increase in membrane conductance produced by the sustained opening of the Na_V and Ca_V channels mediating the PIC (Binder et al., 2020). In adult decerebrate or intact animals, the tertiary range also exhibits a pronounced hysteresis where the sustained plateau potential mediated by the PIC allows the motoneuron to fire at inputs well below that needed to initially recruit the motoneuron (Bennett et al., 1998; Gorassini et al., 1999; Hounsgaard et al., 1988). This hysteresis in firing reflects how much the PIC contributes to the self-sustained firing of the motoneuron and can be measured by the reduction in current injected into the soma at the offset of motoneuron firing (de-recruitment) compared to the higher current required to initiate firing at recruitment (ΔI) (Bennett, Li, Harvey et al., 2001; Gorassini et al., 2004; Li et al., 2004; Powers et al., 2008). In wild-type mice, ΔI remains stable from adolescence (4–9 weeks) to adulthood (13–17 weeks) (Huh et al., 2021); however, these measures were made under pentobarbital anaesthesia where PICs can be suppressed.

During human development, it is not known whether motoneuron PICs also increase in amplitude and decrease in recruitment threshold in the first few weeks and months after birth or whether there are continual changes from preadolescence to adulthood. To address the latter question, we used the simultaneous firing behaviour of multiple motor units from the tibialis anterior (TA) muscle to indirectly examine the potential contribution of motoneuron PICs to self-sustained firing in participants between the ages of 7–17 years in the preadolescent and adolescent stages (Brix et al., 2019; Wood et al., 2019) and during young adulthood (18–28 years of age). These two groups were also compared to an adult group (32–53 years) before appreciable motor unit loss (McNeil et al., 2005) or decreases in self-sustained firing of motor units (Hassan et al., 2021; Orssatto et al., 2021). The firing rate profile of low threshold (control) TA motor units activated during a triangular isometric dorsiflexion were used to estimate the synaptic input to higher threshold (test) motor units (Afsharipour et al., 2020; Gorassini et al., 2002a). Similar to the hysteretic current measurements described above (ΔI), we calculated the difference in the estimated synaptic input needed to terminate firing of the test unit (control unit firing rate, F_T), compared with the synaptic input needed to recruit firing (control unit firing rate, F_R). Thus, the resulting variable, $\Delta F = F_R - F_T$, was employed as a measure of the self-sustained (hysteretic) firing of the motor unit, potentially mediated by a PIC.

Interestingly, the firing rate profiles of human motor units activated during a slow increase in voluntary effort, and presumably synaptic drive, also display an initial acceleration followed by a shallower increase in firing rate (Afsharipour et al., 2020; Beauchamp et al., 2023; Binder et al., 2020), similar to the secondary and tertiary ranges observed in animal motoneurons in response to a slowly increasing somatic current injection. Thus, we fit two straight lines to the ascending portion of the TA motor unit firing profile to delineate the initial firing rate acceleration during the presumed activation of the PIC (secondary range) and the more gradual increase in firing rate following full PIC activation during the tertiary range. We hypothesized that a steep and brief secondary range is produced by a subthreshold activation of a PIC that is accelerating rapidly at the time of motoneuron recruitment compared to a shallower and longer secondary range mediated by a more suprathreshold PIC that is activating more gradually during motoneuron recruitment (Afsharipour et al., 2020). Thus, we measured both the slope and duration of the secondary range to estimate whether there are any differences in the activation threshold of the PIC during development. The slope and duration of the tertiary range was also compared between age groups to estimate whether there were any changes in the firing gain of the motoneuron.

The general excitability of TA motoneurons was also examined across development by measuring the discharge rates of the motor units at different points along the firing rate profile. For example, we examined whether higher start rates were associated with a steeper secondary range slope where a fast accelerating, subthreshold PIC should produce a larger jump in initial firing rates compared to a more gradually activating PIC activated near recruitment. Maximum firing rates were quantified to determine whether they were higher in potentially smaller motoneurons of children as a result of greater input resistance (Jean-Xavier et al., 2018) and shorter after-hyperpolarization potentials (AHP) (Piotrkiewicz et al., 2007). We also examined whether firing rates decreased with increasing recruitment threshold of the motor units, a phenomenon known as an onion skin effect (De Luca & Erim, 1994), given the conflicting findings in the

literature, with some studies showing an onion skin effect in the TA (De Luca & Hostage, 2010) and others not (Erim et al., 1996; Jesunathadas et al., 2012). Lastly, we examined the end firing rates at de-recruitment of the motor units given that very low firing rates during periods of low synaptic drive can be produced by strong, regenerative activation of the NaPIC (Gorassini et al., 2004; Li et al., 2004).

The increased amplitude and persistence of motoneuron PICs during early development in animals may be mediated by a maturation of descending neuromodulatory inputs, such as serotonin or noradrenaline, to the ventral spinal cord (Bregman, 1987; Hounsgaard et al., 1988; Perrier et al., 2013; Xia et al., 2017). Both these neuromodulators work through Gq-protein coupled receptors, such as 5-$HT_{2B/C}$ and $\alpha 1$ (Murray et al., 2010; Murray et al., 2011), which activate protein kinase C to subsequently phosphorylate and facilitate the Na_V and Ca_V channels that contribute to the PIC (Mizuno & Itoh, 2009; D'Amico et al., 2014; Perrier et al., 2013). In adult humans, a single oral intake (20 mg) of selective serotonin reuptake inhibitors (SSRIs), such as citalopram or escitalopram, probably increases serotonin in the spinal cord and is associated with increases in indirect measures of PIC-mediated, self-sustained firing in spinal motoneurons (D'Amico et al., 2013; D'Amico et al., 2014; Murray et al., 2010; Thompson & Hornby, 2013; Wei et al., 2014). Because some participants in the young development and young adult groups were taking SSRIs daily, such as escitalopram, sertraline or fluoxetine (see doses in Methods) to treat various affective and anxiety disorders (Dwyer & Bloch, 2019), we treated these participants as a separate group given the potential effect increased spinal levels of serotonin may have on the threshold and amplitude of the PIC (Harvey et al., 2006a; Li et al., 2007).

Across the age span of 7–53 years, we hypothesized that younger participants (<18 years) would have higher firing rates and greater amounts of self-sustained firing (ΔF), potentially from smaller motoneurons and larger PICs, respectively, compared to older participants (>18 years). The larger PICs may partly be a result of lower levels of spinal inhibition in the younger participants (Geertsen et al., 2017; Willerslev-Olsen et al., 2014), which reduces the amplitude and persistence of the PIC (Bennett et al., 1998; Hyngstrom et al., 2007). Similarly, we hypothesized that participants taking oral SSRIs would have higher initial (start) rates, steeper secondary range slopes and larger amounts of self-sustained firing given that serotonin both reduces the threshold, and increases the amplitude, of the PIC (Harvey et al., 2006a; Li et al., 2007). Lastly, we estimated the skill in producing the triangular dorsiflexion contractions that were used to measure ΔF by quantifying the amount of force steadiness (coefficient of variation of the detrended torque trace) (Skinner et al., 2019) and examined whether it changed during development along with changes in motoneuron excitability.

Methods

Ethical approval and participants

Experiments were approved by the Health Research Ethics Board of the University of Alberta (Protocol 00 076790) and conformed to the Declaration of Helsinki. All 50 participants provided their written informed consent prior to the experiment. The young development group had a mean ± SD age of 12.18 ± 2.69 years (range 7–17 years) with 12 males and eight females ($n = 20$), the young adult group had mean ± SD age of 22.61 ± 3.60 years (range 18–28 years) with six males and seven females ($n = 13$) and the adult group had a mean ± SD age of 42.38 ± 7.92 years (range 32–53 years) with three males and five females ($n = 8$). A separate group of participants were on selective serotonin reuptake inhibitors (SSRI group) and were between the ages of 11 and 28 years (17.02 ± 5.02 years), with four females and five males ($n = 9$). Four of the SSRI participants were taking a daily 10 mg oral dose of escitalopram, three were taking a daily 25 mg ($n = 1$) or 100 mg ($n = 2$) oral dose of sertraline and two were taking a daily 10 mg oral dose of fluoxetine for at least 2 months before the experiment. This SSRI group was compared to their peers (i.e. SSRI control group), also aged between 11 to 28 years (18.17 ± 5.32 years; $P = 0.584$, Mann–Whitney rank sum test) who were not taking SSRIs and comprised 12 females and 14 males ($n = 26$) from the young development and young adult groups. All participants were excluded for any history of central or peripheral nerve injury or disease. Puberty, menstrual or menopausal status were not recorded. In six of the adult participants, parts of the data were taken from a previous study (Afsharipour et al., 2020).

EMG recordings

To isolate single motor units, flexible high-density surface EMG (HDsEMG) electrodes with 64 recording sites (GR08MM1305; OT Bioelecttronica Inc., Turin, Italy) were placed over the TA muscle. The recordings sites, arranged in a 5 (wide) by 13 (long) grid with 8 mm spacing, were placed lengthwise ∼1 cm lateral to the tibia and 4–5 cm below the lower edge of the patella over the belly of the TA muscle. Recordings were made in a monopolar configuration with the reference and ground electrode straps (WS2; OT Bioelecttronica Inc.) wrapped around the lower leg just above the ankle, with the ground strap most distal. To reduce impedance, the skin was first rubbed with an abrasive paste (Nuprep; Weaver and

Company, Denver, CO, USA) and any excess was removed with a saline or alcohol-soaked gauze. HDsEMG signals were amplified (150 times) and filtered with a 10 Hz high pass and 900 Hz low pass filter using a Quattrocento amplifier (16 bit; OT Bioelecttronica, Inc.). A pair of Ag-AgCl surface EMG electrodes (3.2 cm by 2.2 cm; Kendall; Chicopee, MA, USA) were placed in a bipolar configuration over the soleus to measure antagonist muscle activity during the isometric contractions. All signals were digitized and sampled at a frequency of ∼2048 Hz with the Quattrocento A/D.

Experiment protocol

Participants sat in a chair with their knee extended to ∼120° and their dominant foot tightly sandwiched between two plates of an adjustable 3-D printed foot holder, with the heel on the floor and ankle at ∼90°. Dorsiflexion torque was measured by an S-shaped strain gauge (150-lb SSM; Interface Force Measurement Solutions, Scottsdale, AZ, USA) attached to the bottom of the foot holder directly underneath the metatarsophalangeal joint. The maximum dorsiflexion torque was measured from the largest of two maximum voluntary contractions (MVCs) separated by at least 30 s. Participants were then tasked to perform an isometric triangular dorsiflexion at either 10%, 20% or 30% of their MVC torque, and match their torque output to a target triangle presented over a computer screen with the exerted torque being displayed from left to right. Each triangular contraction consisted of a 10 s ascending phase and a 10 s descending phase, with 20 s between each contraction to avoid frequency-dependent facilitation of motor units (Gorassini et al., 2002b). At least eight to 10 contractions were performed at each level of MVC torque in two trial runs, and the four best trials were selected *post hoc* for analysis. Participants started with a 20% or 30% MVC contraction because these were easier to perform.

Data analysis

Decomposition of single motor units. The HDsEMG signals were first converted into a MATLAB file format (MATLAB, version R2021b/R2022a; Mathworks, Inc., Natick, MA, USA) with custom-built functions, and then digitally filtered (fourth-order, zero lag Butterworth filter with a bandpass of 10–500 Hz and an additional 60 Hz notch). HDsEMG signals with a poor signal-to-noise ratio were removed (typically two or three of the 64 recorded signals). Blind source separation (Negro et al., 2016) was used to decompose the HDsEMG signals into the contributing single motor units. Only motor unit action potentials with a mean silhouette (SIL) value of 0.85 or higher were used (Negro et al., 2016). The trains of motor unit action potentials (or pulses) were manually edited to remove or add extra pulses to correct too high or too low firing rates, respectively. Only 10% or less of the pulses were modified in a single firing rate profile. A fifth-order polynomial curve was fit to the firing rate profile of each motor unit for subsequent analysis as described below.

Average number of motor units per contraction. In each participant, the number of decomposed motor units in each contraction that met the criteria for selection (see above) was averaged across the four contractions and plotted against the age of the participant. Two straight lines of different slope were then iteratively fit to the data (see section 'Piecewise linear fit' below) to determine which age range had the largest change in the number of decomposed motor units with age.

Distribution of motor unit recruitment thresholds. The recruitment threshold of the motor units was measured as the torque level when the motor unit began firing, expressed as a percentage of the torque at MVC (% MVC). To examine the distribution of motor units with different recruitment thresholds for each group, the total number of motor units (count) within a range of recruitment thresholds (e.g. bins of 0–5% MVC, 5–10% MVC, etc.) for all four contractions in each participant was pooled within each group. Each bin count was then divided by the number of participants in each group and plotted as a histogram. Note that the different number of decomposed motor units between the various groups, or their distribution according to recruitment threshold, may not represent physiological differences in motor unit numbers or types. Rather, differences in muscle geometry (e.g. size) and/or subcutaneous tissue between the different groups may affect the isolation of single motor units from HDsEMG and blind source decomposition (Oliveira et al., 2022).

ΔF. The contribution of the PIC to self-sustained firing of motoneurons was estimated as per Afsharipour et al. (2020). First, to estimate the synaptic input to the TA motoneuron pool, the firing profiles of the lowest threshold motor units (typically two to five units with recruitment thresholds <3% MVC), were superimposed to produce a composite profile as an average measure of the synaptic drive to the TA motoneuron pool. Abrupt accelerations in firing rate at the onset of the composite firing rate profile (i.e. secondary range) were manually removed so that only the tertiary range remained, which we propose provides a more linear estimate of the synaptic drive to the TA motoneurons. A fifth-order polynomial line was then fitted to the composite profile. In the remaining higher-threshold (test) motor units that were activated for at least 1 s before peak torque, the firing rate

of the composite profile (measured from the polynomial line) when the test unit was de-recruited or terminated (F_T) was subtracted from the firing rate when the test unit was initially recruited (F_R) to produce a ΔF value ($\Delta F = F_R - F_T$). Thus, ΔF is an estimate of the reduction in synaptic input present at recruitment that is needed to terminate motor unit firing to counteract the added depolarization provided by the motoneuron PIC. The continued firing at synaptic levels below recruitment is termed 'self-sustained firing'. An average ΔF across all test motor units was obtained from the four contractions in each participant and plotted across age in the young development and young adult groups. ΔF was also averaged across participants within each group and compared across the different groups.

Self-sustained firing duration (SSD). The SSD may provide another measure of self-sustained firing of the motoneuron. SSD is the percentage of time a motor unit fires on the descending phase of the contraction that is below the level of torque needed on the ascending phase to initially recruit the motor unit (Afsharipour et al., 2020). In this case, the torque profile is used as a rough measure of synaptic input to the motoneuron. To calculate SSD, the formula below is used where 'duration of ascending phase' = the duration of time the test unit was active on the ascending phase of the contraction and the 'duration of descending phase' = duration of time the test unit was active on the descending phase:

$$\mathrm{SSD} = \frac{(duration\ of\ descending\ phase - duration\ of\ ascending\ phase)}{(duration\ of\ descending\ phase + duration\ of\ ascending\ phase)} \times 100\%$$

Thus, a motor unit that fired for 10 s on the descending phase of the contraction, but for only 5 s on the ascending phase (i.e. 5 s longer than expected if the motor unit was de-recruited at the same input as during recruitment), would have a SSD of 33%.

Composite modulation depth (CMod). To measure the excursion (modulation depth) in the firing rate of the composite profile that was used to measure the ΔF, the minimum value of the fit polynomial line on the descending phase of the contraction was subtracted from the maximum value (CMod). This was carried out to ensure that any differences in ΔF between groups were not the result of a small CMod constraining the ΔF values.

Piecewise linear fit to the ascending firing rate profile (three-slope analysis). The firing rate profiles during the ascending portion of the contraction exhibited a non-linear shape with roughly three distinct ranges (slopes) that may arise from the activation of motoneuron intrinsic conductances. We approximated this non-linear response by three connected straight lines of different slopes using the unconstrained MATLAB simplex search method called fminsearch. The first range is a rapid increase in motor unit firing at the onset of the contraction (termed secondary range), probabaly as a result of the activation of the motoneuron PIC at recruitment (Afsharipour et al., 2020; Binder et al., 2020) and we approximated this with a fixed line. After full PIC activation, the firing rate of the motor unit increases more slowly (termed the tertiary range), which we model with a second joined line of lower slope. During the tertiary range, where we presume synaptic drive is still increasing, motor unit firing can decrease before peak torque is reached. We refer to this as the tertiary sag range and these data will be presented in a future paper. To fit a piecewise linear model to the secondary, tertiary and tertiary sag ranges, we employed a non-linear search for parameters m_1 – m_3 (slopes) and b_1 – b_3 (offsets) of three linear equations:

$$\begin{aligned} F(t) &= m_1 t + b_1 \text{ if } t < t_{BP1} \ (\text{Secondary range}) \\ F(t) &= m_2 t + b_2 \text{ if } t_{BP1} < t < t_{BP2} \ (\text{Tertiary range}) \\ F(t) &= m_3 t + b_3 \text{ if } t > t_{BP2} \ (\text{Tertiary sag range}) \end{aligned}$$

where $F(t)$ is the model firing rate and t is time. These lines are constrained to be joined at two breakpoints in time, t_{BP1} and t_{BP2}, because we do not see discontinuities in firing at the transitions between ranges. Thus, $F(t_{BP1}) = m_1\ t_{BP1} + b_1 = m_2\ t_{BP1} + b_2$ and thus, by rearranging we compute:

$t_{BP1} = (b_1 - b_2) / (m_1 - m_2)$ and similarly for the second breakpoint
$t_{BP2} = (b_2 - b_3) / (m_2 - m_3)$

The six unknown parameters (m_1, m_2, m_3, b_1, b_2 and b_3) in this function $F(t)$ were determined iteratively by minimizing the least squared error between the model and actual firing rates, starting with initial guesses (values) for the breakpoints, and using the unconstrained MATLAB simplex search method called fminsearch. Initial guesses for the m and b parameters were obtained by separate linear regressions on the segments of data between the breakpoint values. Because of the non-linear nature of this model (with variable breakpoints), there are multiple

possible solutions (at minima in criteria) depending on the starting initial values given to the breakpoints. We systematically searched the solution space by testing all possible initial values for t_{BP1} and t_{BP2} pairings at each frequency point. Many nearby initial values converged onto a single solution with a common minimum error, and we manually chose the final solution with both the near minimum error and the largest number of initial value pairs that led to that error. Sometimes two or more such solutions arose, and we chose the one that best fit the bin averaged (10 ms bins) firing rate profile, as determined visually. Final solutions were also constrained to have a positive secondary range slope that was at least twice as steep as the tertiary range slope and a tertiary sag range with a slope <0 Hz s^{-1}. If there was no secondary range (i.e. $b_1 < 2\ x$'s b_2), the firing rate profile was fit with just one or two straight lines to delineate the tertiary range only or the tertiary and tertiary sag ranges, respectively. In many of the higher threshold units when there was no period of low slope firing that was similar to the tertiary range observed in the lower threshold units, we also fit one or two lines to the firing rate profile to delineate the secondary range only or the secondary and tertiary sag ranges, respectively. Finally, in cases where there was no tertiary sag range, the straight line through the tertiary range was extended to the peak torque to measure its slope and duration.

The proportion of motor units exhibiting a secondary and/or tertiary range was calculated in each participant by first binning the motor units according to their recruitment threshold (see below) and pooling all of the motor units from the four contractions together. The percentage of total units in each bin with a secondary or tertiary range was then calculated (e.g. number of units with a secondary or tertiary range/number of total units within the bin $\times$ 100%) and this percentage was then averaged across participants within each group for each bin. The slope and duration of the secondary and tertiary ranges were also analysed like ΔF with respect to age (see above) and the recruitment threshold of the motor units (described below).

Start, maximum and end rates. The start, maximum or end firing rate for all units in each contraction were measured from the fit polynomial line using a custom MATLAB program. The average value measured from all units in a single contraction was calculated and this value was then averaged across the four contractions in each participant and then across participants within a group. The mean start, maximum and end firing rates were also plotted against the age of the participant in the young development and young adult groups (7–28 years) to visualize trends across age and across the recruitment threshold of the motor units.

Antagonist muscle activation. Because the firing rate profiles of the TA motor units could be affected by a counter load produced from antagonist muscle activation, we used MATLAB to measure the mean rectified and smoothed (fourth-order, zero lag Butterworth filter with 30 Hz low pass) soleus EMG during the entire triangular dorsiflexion. The mean noise of the signal, measured before or after the contraction with no EMG activity, was subtracted to better compare soleus EMG values across the different participants. The mean amplitude of the soleus EMG during the 30% MVC triangular contraction was compared with the mean soleus EMG produced during the less controlled, dorsiflexion MVC where, in the latter, we expect a greater amount of co-contraction.

Onion skin effect. As noted in the Introduction, the onion skin effect can present when the mean (and by extension the maximum) firing rate decreases with the recruitment threshold of the motor units (De Luca & Hostage, 2010; Erim et al., 1996). To determine whether this effect occurred in the TA motor units for our recording and decomposition protocol, in each participant, the maximum firing rate of each motor unit was plotted against its recruitment threshold, grouping data from all four contractions together and calculating repeated measures correlation coefficients (*rmcorr*). Briefly, *rmcorr* avoids violating the assumption of independence of observations by using analysis of covariance to statistically adjust for inter-individual variability and generating the best linear fit for each participant using parallel regression lines (the same slope) with a unique intercept (Bakdash & Marusich, 2017). The *rmcorr* can range from -1 to 1 and indicates the strength of the linear relationship between two variables, similar to a Pearson correlation coefficient, with *rmcorr* of $|0.10|$, $|0.30|$ and $|0.50|$ considered to have small, medium and large effect sizes respectively (Bakdash & Marusich, 2017).

Analysis according to recruitment threshold of the motor units. To examine whether the ΔF, secondary and tertiary range or firing rate values varied according to the recruitment threshold of the motor units, values from motor units having a recruitment threshold within a given range (e.g. bins of 0–3%, 3–5%, 5–7%, … 25–27% MVC) from the four contractions were averaged together in each participant using a custom MATLAB program. These binned averages were then averaged across participants within each group to compare between different group pairings (e.g. young development *vs.* young adult, SSRI *vs.* SSRI control, etc.).

Torque steadiness and motor unit interspike interval. Torque steadiness was quantified by measuring the coefficient of variation (CoV) of the detrended torque

trace. In each participant, the four triangular torque ramps were subjectively split into ascending and descending components, determined visually as the point where the torque transitioned from an ascending to a descending profile near its peak. The MATLAB detrend function was applied to the separated ascending and descending components where the best straight-line fit to the data was removed. The SD of the detrended torque was calculated across the entire ascending or descending phase. The SD of the ascending or descending detrended torque was then divided by the mean of the non-detrended torque to produce the CoV (SD/mean) (Skinner et al., 2019). Note that the homoscedasticity of the SD across the ascending or descending phase was not measured and was probably greater near peak torque compared to the onset of the contraction. However, because we are only using CoV as a measure of torque variability, this was not a large concern. The CoV of the interspike interval for the motor unit discharge times was also measured in the young development and young adult groups to determine whether it followed a similar trend across age similar to the CoV of the detrended torque. The SD and mean interspike interval across the entire ascending and descending discharge profile for each motor unit was measured to calculate the CoV (SD/mean). In each participant, the CoV of the interspike interval for all motor units from all four contractions was pooled and then averaged together to obtain a single CoV value and plotted against age.

Statistical analysis

Sigma Plot, version 11.0 (Grafiti LLC, Palo Alto, CA, USA), was used for all statistics except for the repeated measures correlation coefficients described below. Because the group ΔF and mean firing rates did not differ between males and females during the 30% MVC contractions, as will be detailed elsewhere, data from the two sexes were collapsed within each group. A Shapiro–Wilk test was used to assess the normality of the data. Group comparisons consisted of young development *vs*. young adult, young development *vs*. adult, young adult *vs*. adult and SSRI *vs*. SSRI controls. Unpaired, between-group comparisons for normally distributed data were assessed with Student's *t* test and non-parametric data were assessed with the Mann–Whitney rank sum test. The relationship between the different dependent variables (i.e. ΔF, CMod, SSD, secondary and tertiary range slopes and durations, firing rates and torque steadiness) and the age of the participant was evaluated with a Pearson product correlation moment (r). Within each group, a one-way analysis of variance (ANOVA) was performed on normally distributed data and a one-way ANOVA on ranks was used on non-normally distributed data to compare the effect of motor unit recruitment threshold on the ΔF, secondary and tertiary range slope and duration, and the various firing rates. A two-way ANOVA was also performed to analyse the effect of group and recruitment threshold and their interaction on these different variables. To examine maximum firing rates across the recruitment threshold of the motor units, repeated measures correlation coefficients were calculated independently for each group using the *rmcorr* package (Bakdash & Marusich, 2017) in R (R studio, version 1.4.1106; R Foundation for Statistical Computing, Vienna, Austria). $P < 0.05$ was considered statistically significant. Data are presented as the mean ± SD or median (range) when appropriate.

Results

Number and firing rate profiles of decomposed motor units

Using the blind-source separation algorithm (Negro et al., 2016), 2164 single motor units from the four contractions were decomposed from the TA HDsEMG activated during the 30% MVC dorsiflexion, with 575 units decomposed in the young developmental group (aged 7–17 years, $n = 20$), 669 units in the young adult group (aged 18–28 years, $n = 13$), 384 units in the SSRI group (aged 11–28 years, $n = 9$) and 536 units in the adult group (32–53 years, $n = 8$). In all groups, the average pulse-to-noise ratio, or silhouette (SIL) value, was greater than the cutoff of 0.85 (young development = 0.89 ± 0.023; young adult = 0.90 ± 0.030, SSRI = 0.900 ± 0.018 and adult group = 0.94 ± 0.025). Example motor unit firing profiles with the fit polynomial lines (black) from a single 30% MVC contraction are shown in Fig. 1 for an 11-year-old in the young development group, a 19-year-old in the young adult group and from a 16-year-old taking an SSRI; for similar data in adults, see Afsharipour et al. (2020). All ten decomposed motor units are displayed for the 11-year-old and are plotted in order of increasing recruitment threshold, whereas 10 representative motor units with similar increments in recruitment threshold are displayed for the other two participants. The motor unit firing rate profiles of the 11-year-old participant were similar to the participant taking SSRIs and distinct from the older 19-year-old participant. For example, firing rates were more variable in the young development and SSRI participants and reached higher maximum rates compared to the young adult participant, with the latter reflected by a greater number of polynomial lines crossing above the coloured vertical lines. Moreover, motor units recruited at torques of ∼10% MVC or higher continued to fire for longer as the dorsiflexion torque (Fig. 1, top trace) decreased towards zero at the end of the contraction (Fig. 1, vertical dotted line), especially in the SSRI participant compared to the young adult, suggesting

that these motor units had greater amounts of prolonged, self-sustained firing.

When first comparing across all participants, the average number of motor units decomposed per contraction increased more steeply with age up until ∼30.25 years as measured by fitting two straight lines to the data (Fig. 2*A*, SSRI participants in red). On average, there were more units decomposed per contraction in the young adult (12.86 ± 7.65) and adult (16.75 ± 6.40) groups compared to the young development (7.03 ± 3.67) group ($P = 0.041$ and 0.021, respectively, Mann–Whitney rank sum test), with no difference in the young adult and adult groups compared to the SSRI (10.66 ± 5.96) group ($P = 0.479$ Student's t test and $P = 0.295$, Mann–Whitney rank sum test, respectively). Moreover, the young adult and adult participants had a greater proportion of lower-threshold units (i.e. peak of gaussian curve at 2.5% MVC) (Fig. 2*B*, middle) compared to the young

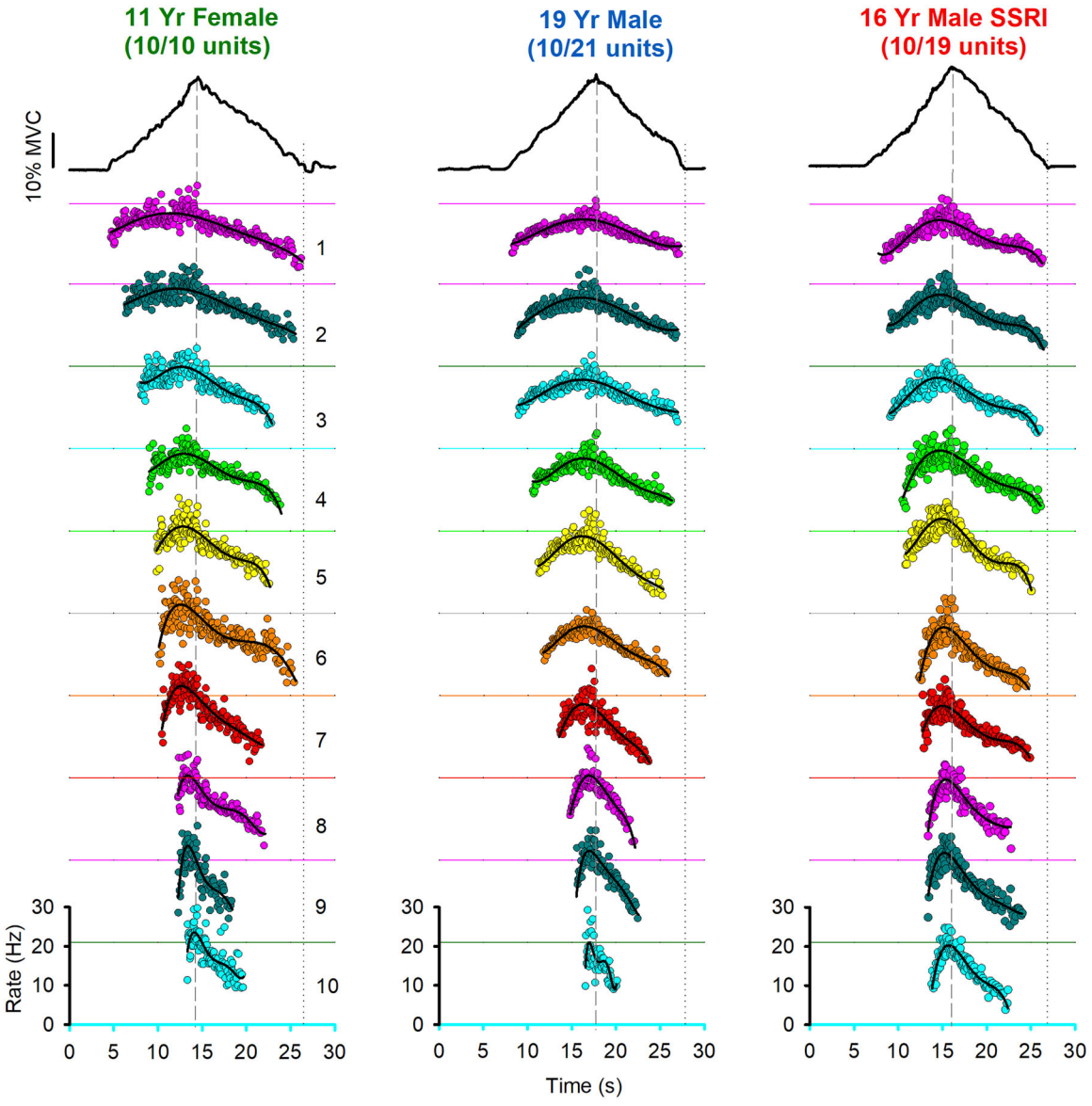

Figure 1. Dorsiflexion torque (top trace) and firing rate profiles of 10 decomposed TA motor units during a triangular 30% maximum voluntary contraction (MVC) plotted from top to bottom in order of increasing recruitment threshold
Left: 11-year-old female (10 out of 10 units decomposed). Middle: 19-year-old male (10 out of 21 units). Right: 16-year-old male taking an SSRI (10 out of 19 units). The vertical long dashed lines mark the time of peak torque and the dotted lines mark the time of zero torque at the end of the contraction. The black lines show the fifth-order polynomial fit to the firing rate profiles. The 0 Hz baseline (x-axis) is displayed in the corresponding colour for each motor unit, except for the yellow units where grey is used to improve visibility. [Colour figure can be viewed at wileyonlinelibrary.com]

development group (peak at 7.5% MVC) (Fig. 2*B*, top left) and the participants taking SSRIs (peak at 12.5% MVC) (Fig. 2*B*, bottom right). Because the distribution of recruitment thresholds in the decomposed motor units was different across groups, in addition to age we also plotted ΔF and other measures across the recruitment threshold of the motor units to determine whether it was a contributing factor.

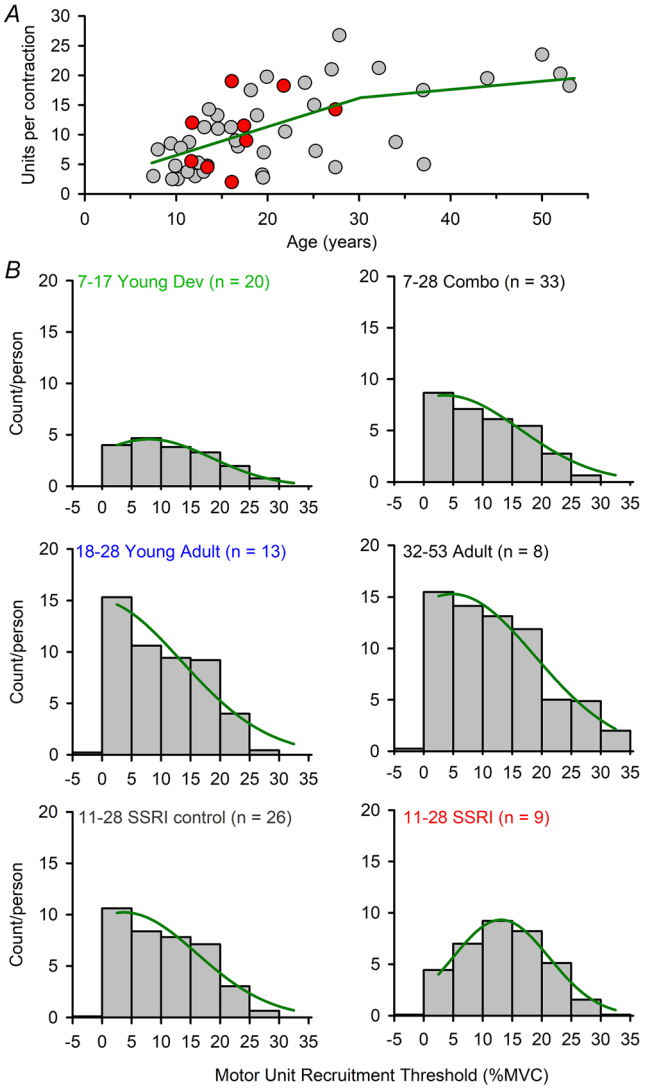

Figure 2. Mean number and recruitment threshold distribution of motor units
A, mean number of TA motor units per contraction plotted against the age of the participant. Participants taking SSRIs are marked with red circles. Two lines of different slope (green) with the smallest error were iteratively fit to the data. *B*, histogram distribution of number of motor units binned according to the recruitment threshold of the motor unit (in increments of 5% MVC) and divided by the number of participants in each group. The combined young development and young adult group (Combo: 7–28 years) is also displayed. *N*, number of participants in each group. [Colour figure can be viewed at wileyonlinelibrary.com]

Estimation of self-sustained firing

ΔF was measured to estimate whether there were changes in self-sustained firing of motoneurons across development and whether it was larger in participants taking SSRIs. To measure ΔF, the profile of the synaptic input to the TA motoneurons was estimated by averaging the mean firing rate profile of the two or three lowest-threshold control units (e.g. bottom profiles in Fig. 3*A* with grey, light blue and green dots) to produce a composite control motor unit profile as per Afsharipour et al. (2020). This estimated synaptic input was typically lower when the test motor units (orange dots, top profiles) were de-recruited compared to when they were first recruited (ΔF marked by length of downward arrows in Fig. 3*A*), potentially from the added depolarization of the PIC assisting self-sustained firing at low synaptic inputs. ΔF was larger in both the young development (7.1 Hz) and SSRI (9.3 Hz) participants compared to the young adult participant (4.6 Hz), consistent with the motoneuron PIC in the former two groups producing greater amounts of self-sustained firing.

To explore the relationship of age to ΔF further, we plotted the mean ΔF for each of the young development and adult participants across age and noted a negative correlation as marked by the black regression line ($r = -0.496$, $P = 0.006$, Pearson's product), showing that ΔF decreases with age from 7 to 28 years (Fig. 3*Ba*). Correspondingly, the average ΔF in the young development group (5.83 $\pm$ 1.15 Hz) (Fig. 3*Ca*) was larger than the young adult group (4.88 $\pm$ 0.80 Hz, $P = 0.015$, Student's t test) and the adult group (4.78 $\pm$ 1.05 Hz, $P = 0.035$, Student's t test) (for t values, see Supporting information, Table S1b). Moreover, the average ΔF was higher in the SSRI group (6.45 $\pm$ 0.56 Hz) (Fig. 3*Ca*) compared to the age-matched controls (5.27 $\pm$ 1.05 Hz, $P = 0.003$, Student's t test; see also Supporting information, Table S1b).

The larger ΔF in the young development and SSRI groups could have been mediated by a greater excursion in firing rate modulation of the composite control motor units (CMod, lower profiles in Fig. 3*A*). However, unlike ΔF, CMod in the young development (11.22 $\pm$ 2.09 Hz) (Fig. 3*Cb*) was not larger compared to the young adult (10.17 $\pm$ 1.66 Hz, $P = 0.139$) or adult groups (10.94 $\pm$ 3.28 Hz, $P = 0.787$, Student t tests), nor were there differences between the SSRI group (11.88 $\pm$ 0.99 Hz) and the age-matched controls (10.62 $\pm$ 1.97 Hz, $P = 0.076$, Student's t test), with CMod being almost twice that of the ΔF values. Moreover, there was no relationship between CMod and age across the young development and young adult groups as marked by the grey regression line in Fig. 3*Bb* ($r = -0.166$, $P = 0.357$, Pearson's product). A similar CMod across groups suggests that the lower ΔF in the young adult

and adult groups were not constrained by a lower CMod. The smaller number of decomposed TA motor units in the young development group (Fig. 2) also could have biased sampling to produce a higher ΔF. However, when comparing ΔF to a group of young adults and adults ($n = 10$) with a similar number of decomposed motor units per contraction (median number of units = 7.13) compared to the young development group (median: 7.50, $P = 0.704$ Mann–Whitney rank sum test), ΔF was still larger in the young development group (5.83 ± 1.15 Hz) compared to this combined adult group (4.95 ± 0.99 Hz, $P = 0.035$, Student's t test).

The differences in estimated PIC activation between the three participants from Fig. 3*A* were also reflected in the measure of SSD, which is the percentage of time a motor unit fires below the torque needed to initially recruit the motor unit (Fig. 3*A*, horizontal double arrow) (Afsharipour et al., 2020). The SSD was 54% in the 11-year-old, 21% in the 19-year-old and 47% in the 16-year-old taking an SSRI. However, in the group data (Fig. 3*Cc*), SSD in the young development group (19.44 ± 18.51%) was not larger compared to the young adult (14.74 ± 12.29%, $P = 0.543$) or the adult group (10.52 ± 7.71%, $P = 0.525$, Mann–Whitney rank sum

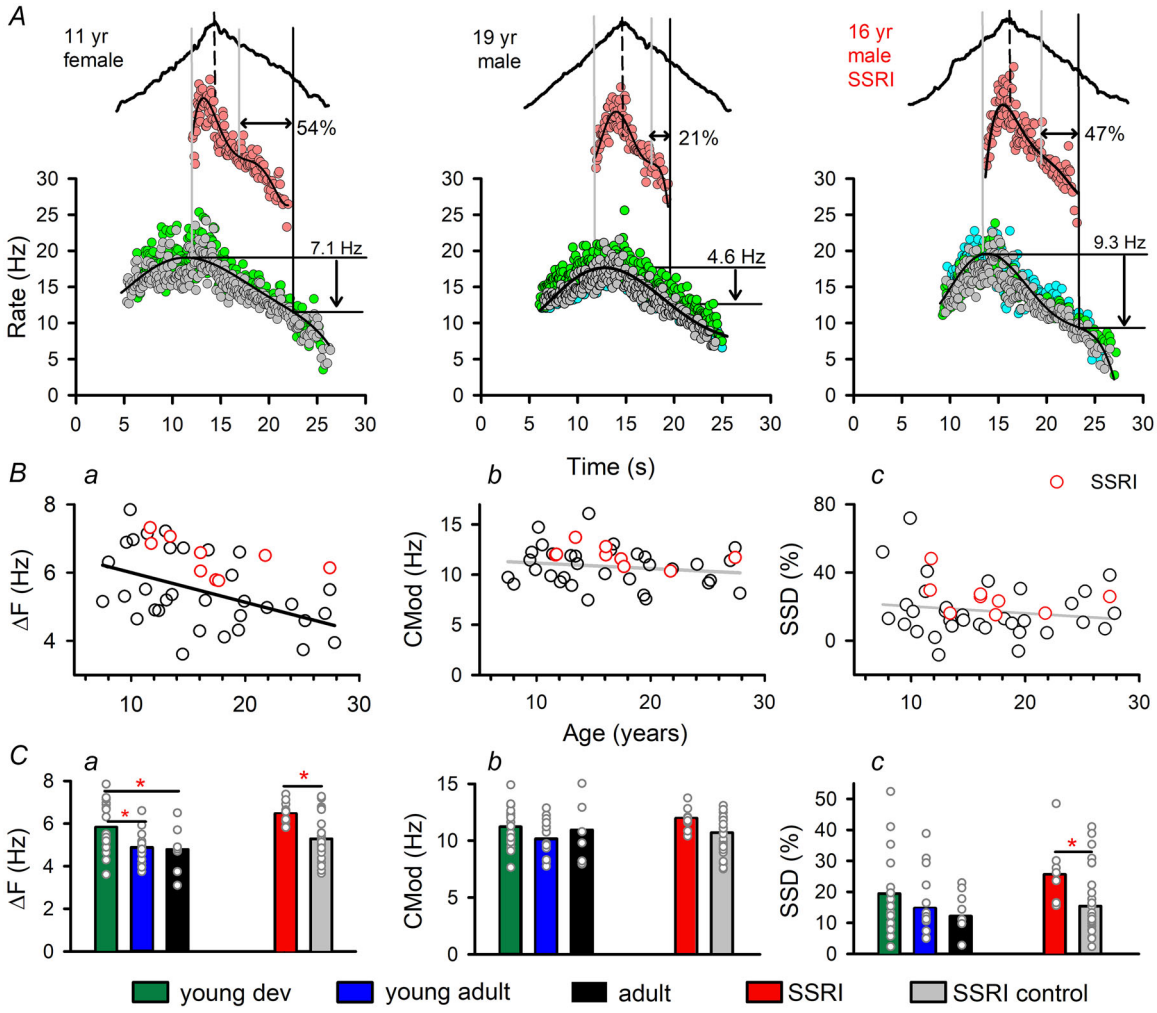

Figure 3. ΔF, Control Unit Modulation Depth (CMod) and Self-sustained firing Duration
A, representative firing rate profiles of composite TA control units (bottom profiles, different control units indicated with different colours) and test units (top profiles, orange) used to measure ΔF, CMod and SSD in the same three participants from Fig. 1. Solid black lines indicate fitted fifth-order polynomial. *B*, ΔF (*Ba*), CMod (*Bb*) and self-sustained firing duration (SSD) (*Bc*) plotted against age across the young development ($n = 20$) and young adult groups ($n = 13$). Black regression lines indicate there is a significant correlation with age; grey regression lines indicate no correlation. Participants taking SSRIs ($n = 9$, not included in regression analysis) are marked with red circles. *C*, height of bar indicates mean ΔF (*Ca*), CMod (*Cb*) and SSD (*Cc*) for the young development (green), young adult (blue), adult (black), SSRI (red) and SSRI control (grey) participants. *Statistical difference between groups with $P < 0.05$; the results of unpaired comparisons are provided in the text and Supporting information (Table S1b). [Colour figure can be viewed at wileyonlinelibrary.com]

test), nor was there a correlation between SSD and age across the young development and young adult groups (Fig. 3*Bc*, grey regression line, $r = -0.149$, $P = 0.407$, Pearson's product). By contrast, SSD in the participants taking SSRIs (25.27 ± 10.12%) was larger compared to the age-matched controls (15.02 ± 12.57%, $P = 0.035$, Student's *t* test), similar to ΔF (Fig. 3*Cc*).

We also examined ΔF as a function of recruitment threshold of the test motor units (Fig. 4) given the different distributions of motor unit recruitment thresholds between the groups (Fig. 2*B*) and the potential for it to affect ΔF (Harris-Warrick et al., 2023; Sharples & Miles, 2021). When tested with a one-way ANOVA, there was no significant main effect of recruitment threshold on ΔF within any of the groups (see one-way ANOVA results in the Supporting information, Table S2a), in agreement with Afsharipour et al. (2020). As with the unpaired comparisons in Fig. 3*Ca*, a two-way ANOVA showed a main effect of group on ΔF between the young development and young adult groups ($F_{1,12} = 24.781$, $P < 0.001$), the young development and adult groups ($F_{1,12} = 21.690$, $P < 0.001$) and the SSRI and SSRI control groups ($F_{1,12} = 24.558$, $P < 0.001$) (see all two-way ANOVA results in the Supporting information, Table S2b).

Proportion of motor units having a secondary and/or tertiary range

Three joined, straight lines of different slopes were fit to the ascending portion of the firing rate profiles to quantify the non-linearities in motor unit firing in response to the presumed linear increase in synaptic drive to the TA motoneurons (see 'Piecewise linear fit' in Methods). The first slope, termed the secondary range (Fig. 5*A*, light blue), is considered to reflect the acceleration in firing rate when the PIC is activated during recruitment of the motoneuron and thus may potentially provide an estimate of the upswing in membrane potential during PIC activation. As shown for the top firing rate profiles in Fig. 5*A*, ∼85–90% of all motor units activated between 0% and 15% MVC had a secondary range (Fig. 5*B*, top graphs plotted for each group), with the remaining units having firing rate profiles that jumped directly onto the tertiary range (e.g. unit 2 from 11-year-old in Fig. 1). As the recruitment threshold of the motor units increased above 18% MVC (e.g. bottom units in Fig. 5*A*), almost 100% of all motor units had a secondary range. The next slope, termed the tertiary range (Fig. 5*A*, green), is considered to reflect the lower gain firing of the motoneuron after the full activation of the PIC increases the conductance of the cell (Bennett et al., 1998). In every group, all motor units recruited between 0% and 5% MVC had a tertiary range (Fig. 5*B*, bottom row), and this proportion rapidly dropped off for motor units with recruitment thresholds >13% MVC when the secondary range started to dominate most of the ascending firing rate profile (e.g. Fig. 5*A*, bottom profiles). There were no differences in the proportion of units with a secondary or tertiary range between the various groups (see two-way ANOVA results in the Supporting information, Table S3).

Secondary and tertiary range slopes and durations

Similar to ΔF and SSD, we first plotted the slope and duration of the secondary and tertiary ranges across the age of the participants. Similar to ΔF, the *slope* of the secondary range decreased with age ($r = -0.387$, $P = 0.026$, Pearson's product) (Fig. 6*A* left), with the young development group having a steeper secondary range slope (5.73 ± 1.93 Hz s^{-1}) (Fig. 6*A*, right) compared to the young adult (4.34 ± 0.90 Hz s^{-1}) and adult

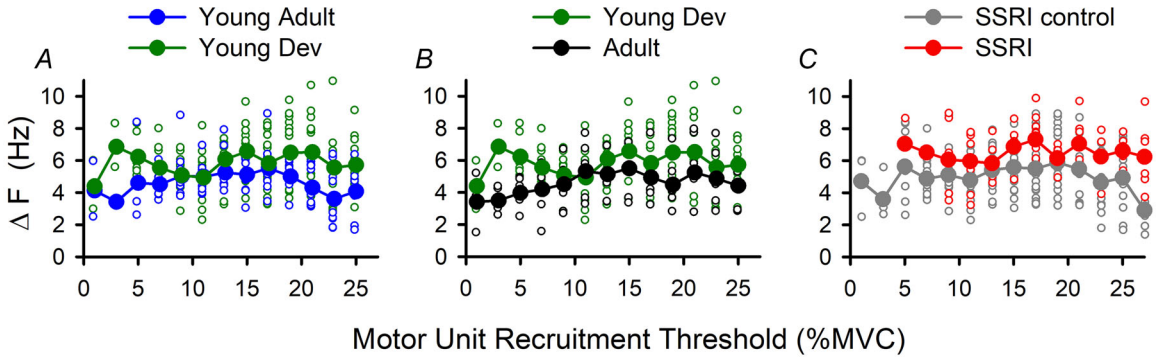

Figure 4. ΔF and recruitment threshold of the test motor unit
ΔF plotted against recruitment threshold of the test motor units (binned every 2% MVC) for *A*, young development ($n = 20$, green) and young adult ($n = 13$, blue) groups; *B*, young development and adult ($n = 8$, black) groups; *C*, SSRI ($n = 9$, red) and aged-match control ($n = 26$, grey) groups. Solid symbols denote a significant group effect from the two-way ANOVA analysis (all results of two-way ANOVA are displayed in the Supporting information, Table S2b). Small circles indicate individual participant data. [Colour figure can be viewed at wileyonlinelibrary.com]

(4.35 ± 1.20 Hz s^{-1}) groups ($P = 0.026$ and $P = 0.050$, respectively, Mann–Whitney rank sum). By contrast, the *duration* of the secondary range did not vary with age across the young development and young adult groups ($r = 0.167$, $P = 0.354$, Pearson's product) (Fig. 6*B*, left), nor were there differences between the young development and young adult or adult groups (Fig. 6*B*, right; see results of unpaired comparisons in the Supporting information, Table S4c). The secondary range slope was steeper in the SSRI group (7.20 ± 2.38 Hz s^{-1}) (Fig. 6*A*, right) and with a shorter duration (1.39 ± 0.25 s) (Fig. 6*B*, right) compared to the age-matched controls (slope: 4.96 ± 1.69 Hz s^{-1}, duration: 1.68 ± 0.32 s, $P = 0.004$ Mann–Whitney rank sum test and $P = 0.019$ Student's t test, respectively). Interestingly, the slope (and sometimes duration) of the secondary range followed a similar trend across the groups as the ΔF estimate of self-sustained firing (as detailed below in Fig. 8). By contrast, there were no associations in

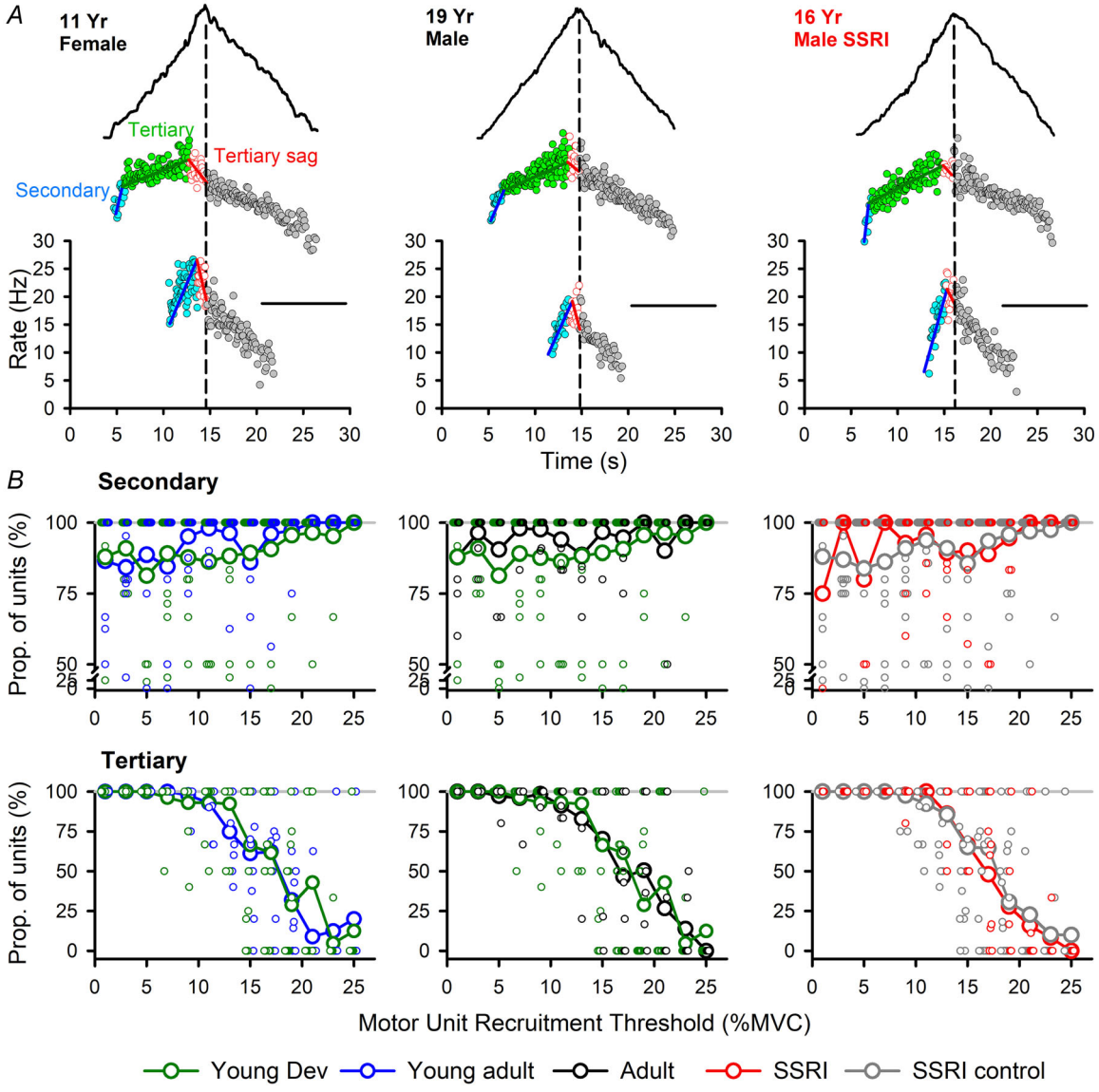

Figure 5. Proportion of motor units with secondary and tertiary ranges
A, examples of secondary (blue), tertiary (green) and tertiary sag (red) ranges fit to the ascending profile of both a lower threshold (middle plot) and higher threshold (bottom plot) motor unit in the same three participants as in Fig. 1. The vertical dashed line marks peak torque and the black horizontal line represents 0 Hz for the top firing rate profiles. *B*, top row: large circles mark mean proportion of units within each 2% MVC bin with a secondary range in the young development (green) and young adult (blue) groups (left); young development and adult (black) groups (middle); and SSRI (red) and age-matched controls (grey) (right). Small circles mark individual participant values with overlapping data points (e.g. at 100% proportion) skewed slightly to the left or right of the bin centre (e.g. 1%, 3% and 5% MVC, etc.). Bottom row: Same as for the top row but for the tertiary range. [Colour figure can be viewed at wileyonlinelibrary.com]

the slope (~0.6 Hz s^{-1}) or duration (~5 s) of the tertiary range with age where motoneuron firing is asssumed to occur during full PIC activation (grey regression lines in Fig. 6*C* and *D*, left; for *r* values, see Supporting information, Table S4b), nor were there any differences between the various groups (Fig. 6*C* and *D* right graphs; see unpaired comparisons in the Supporting information, Table S4c).

We also examined whether the slope and duration of the secondary and tertiary ranges varied across the recruitment threshold of the motor units within each group (Fig. 7). In general, the slope of the secondary range decreased, and the duration became longer as the recruitment threshold of the motor units increased (marked with an asterisk in Fig. 7*A*, top and bottom, respectively; see one-way ANOVA results in the Supporting information, Table S5), consistent with the threshold of the PIC increasing with the recruitment threshold of the motoneuron as described in the Introduction. By contrast, there was no effect of recruitment threshold on the slope of the tertiary range for any group (Fig. 7*B*, top; see one-way ANOVA results in the Supporting information, Table S5). As expected, there was an effect of recruitment threshold for the duration of the tertiary range because more of the firing rate profile in the higher threshold units was comprised of the secondary range (marked with an asterisk in Fig. 7*B*, bottom; see one-way ANOVA results in the Supporting information, Table S5), with many of the motor units recruited at or above 23% MVC having no tertiary range and only a secondary range as shown in Fig. 5*B*. The filled in circles in Fig. 7 indicate a main effect of group from a two-way ANOVA analysis (see Supporting information, Table S6), with similar results to the unpaired comparisons in Fig. 6.

Correlation between ΔF and slope of the secondary range

The slope of the secondary range exhibited similar trends across age and between the different groups as the ΔF. For example, both the ΔF and the slope of the secondary range decreased with age across the young development and young adult groups and both were greater in the young development group compared to the young adult and adult groups and between the SSRI group and the age-matched controls (compare Figs 3*BaCa* and 6*A*). Thus, we plotted the average slope of the secondary range for each participant against their average ΔF to determine whether they were indeed correlated (Fig. 8). Across the entire group, there was a correlation between ΔF and the slope of the secondary range ($r = 0.536$, $P < 0.001$, Pearson's product $n = 50$), showing that these two estimates of motoneuron PIC activation co-vary with one another.

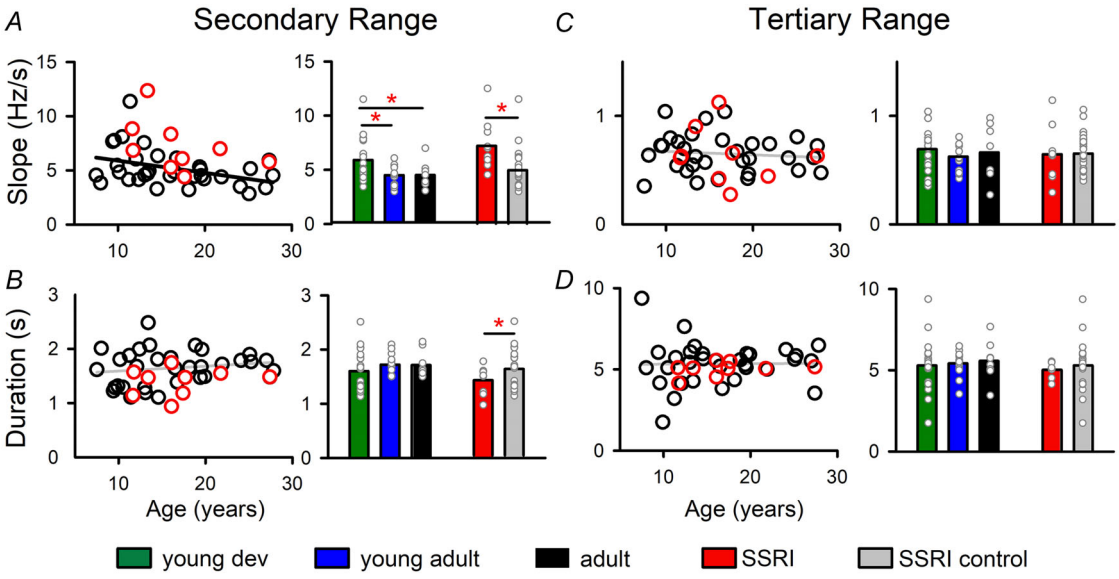

Figure 6. Slope and duration of the secondary and tertiary ranges
Left: mean slope of the secondary (*A*) and tertiary (*C*) ranges plotted against the age of the participants in the young development and young adult groups (black circles, $n = 33$) and participants taking SSRIs (red circles, $n = 9$). Solid black line represents significant regression with age. SSRI participants are not included in the regression. Right: mean slope of secondary (*A*) and tertiary (*C*) range (height of bar) for young development (green), young adult (blue) and adult (black) groups and for SSRI (red) and SSRI-control (grey) groups. Small circles indicate individual participant values. *B* and *D*, as in (*A*) and (*C*) but for secondary and tertiary range duration. *Statistical difference between groups (see values in text and bolded numbers in the Supporting information, Table S4c). [Colour figure can be viewed at wileyonlinelibrary.com]

Torque steadiness

Similar to measures of motoneuron excitability, the steadiness of the dorsiflexion torque when trying to track the target triangle also changed with development as assessed by the coefficient of variation (CoV = SD/mean) of the detrended torque during both the ascending or descending phases of the contraction. Similar to ΔF and the slope of the secondary range, the CoV of the detrended torque, for both the ascending ($r = -0.587$, $P < 0.001$) (Fig. 9*A*, left) or descending ($r = -0.493$, $P = 0.004$) (Fig. 9*B*, left, Pearson's product) phase of the contraction, decreased across age between 7 and 28 years, signifying an improvement in dorsiflexion skill during development. Overall, the CoV of the ascending torque profile in the young development group was larger (0.093 ± 0.036) compared to the young adult (0.059 ± 0.016) and adult (0.057 ± 0.011) groups ($P = 0.002$ and $P = 0.004$,

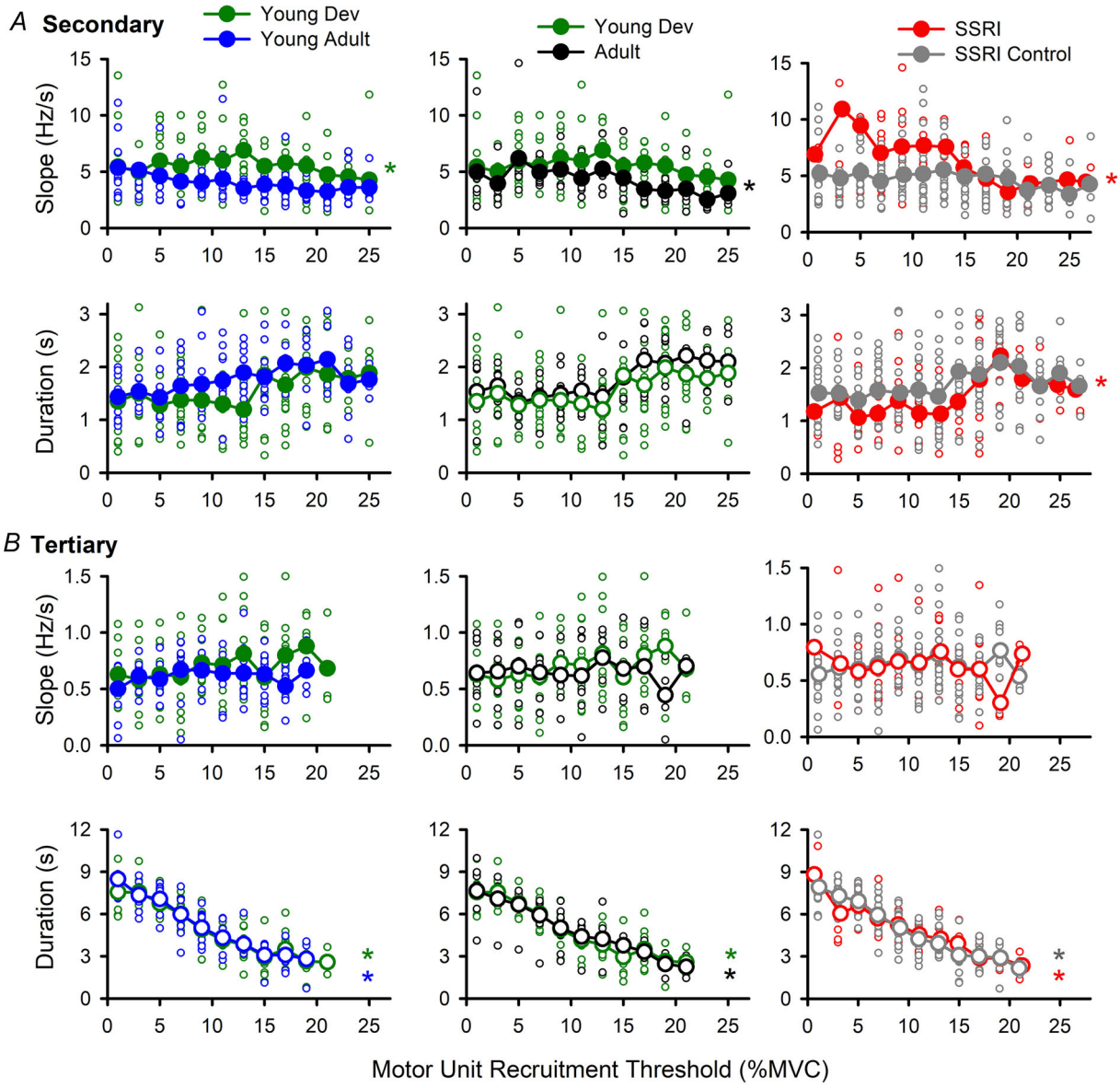

Figure 7. Slope and duration of the secondary and tertiary ranges according to the recruitment threshold of the motor units
A, slope (top) and duration (bottom) of the secondary range plotted against motor unit recruitment threshold (2% MVC bin widths): left: young development *vs*. young adult; middle panels: young development *vs*. adult; right: SSRI *vs*. SSRI controls. *B*, as in (*A*) but for tertiary range. *Statistically significant effect of recruitment threshold on secondary and tertiary range slope or duration from one-way ANOVA colour coded to the respective group (see bold numbers in the Supporting information, Table S5). Solid circles indicate a main effect of group from a two-way ANOVA (see bold numbers in the Supporting information, Table S6). Small circles represent individual participant values. [Colour figure can be viewed at wileyonlinelibrary.com]

respectively, Mann–Whitney rank sum test) (Fig. 9*A*, right). The CoV of the detrended torque during the descending phase of the contraction was also larger in the young development group (0.089 ± 0.034) but only compared to the young adult group (0.067 ± 0.023, $P = 0.041$, Mann–Whitney rank sum test) (Fig. 9*B* right; results of all unpaired comparisons in the Supporting information, Table S7c). By contrast, torque steadiness in the participants taking SSRIs (Fig. 9*A* and *B*, open red circles) was not different compared to the age-matched controls (see values in the Supporting information, Table S7a,c), consistent with a similar level of dorsiflexion skill in the two groups. Similar to the CoV of the detrended torque, the CoV of the interspike interval of the motor unit firing times for the entire firing rate profile also decreased across age ($r = -0.524$, $P = 0.002$, Pearson's product) (Fig. 9*C*, left), with the CoV of the interspike interval in the young development group (0.51 ± 0.09) higher compared to the young adult group (0.43 ± 0.07, $P = 0.018$ Student's *t* test) (Fig. 9*C*, right), signifying that motor unit firing rates were also more variable at ages less than 18 years.

Start, maximum and end firing rates across age

The mean firing rates of the TA motor units activated during a 30% MVC isometric dorsiflexion were often higher in the young development and SSRI groups compared to the adult and SSRI control participants, respectively. As shown for a young development (10 years old) and 21-year-old SSRI participant (Fig. 10*A*, left and right), the maximum and end firing rates of the various motor units were often higher compared to young adults (e.g. 24-year-old) (Fig. 10*A*, middle) and adults (not shown). Across the young development and young adult groups from 7 to 28 years of age, there was a negative correlation between the maximum or end firing rates and age ($r = -0.363$, $P = 0.038$ and $r = -0.484$, $P = 0.004$ respectively, Pearson's product) (Figs 10*Bb* and *Bc*). Moreover, maximum firing rates in the young development group (18.32 ± 2.44) were higher compared to the young adult group (16.51 ± 1.75, $P = 0.028$, Student's *t* test) (Fig. 10*Cb*) and, similarly, the end firing rates in the young development group (7.29 ± 1.64) were higher compared to both the young adult (6.13 ± 1.03) and adult (6.04 ± 0.85) groups ($P = 0.029$ and $P = 0.050$ respectively, Student's *t* test) (Fig. 10*Cc*). By contrast, the start rates in the young development group (10.38 ± 1.95 Hz) were not different compared to the young adult (9.36 ± 1.54 Hz) and adult (9.84 ± 1.98 Hz) groups (P all > 0.05, Student's *t* test) (Fig. 10*Ca*; see statistical results in the Supporting information, Table S8c), nor was there a correlation to age ($r = -0.261$, $P = 0.142$, Pearson's product) (Fig. 10*Ba*). However, both the start (11.18 ± 1.57 Hz) and maximum (19.02 ± 1.98 Hz) firing rates were higher in the SSRI group compared to the age-matched controls: 9.64 ± 1.82, $P < 0.001$ Mann–Whitney rank sum test) (Fig. 10*Ca*) and 17.23 ± 2.26 Hz, $P = 0.042$, Student's *t* test) (Fig. 10*Cb*), respectively.

We examined whether the higher firing rates of the TA motor units in the young development group occurred because of a larger activation of the antagonist soleus muscle that produced a larger counter load to the ankle dorsiflexion. The mean amplitude of the rectified and smoothed soleus EMG during the triangular dorsiflexion contraction was very low in all groups (~2 μV) compared to the soleus activity generated during the less controlled, maximum dorsiflexion contraction (~50 μV). The median rectified and filtered soleus EMG in the young development group was 2.156 μV (range 1.219–2.863 μV) and was not different to the young adult group at 1.773 μV (range 1.342–2.657 μV, Mann–Whitney sum rank test, $P = 0.401$, $T = 2304.000$). Thus, the coactivation of the antagonist soleus muscle probably had little to no effect on the firing rates of the TA motor units or on the other measures of unit firing such as ΔF, secondary and tertiary range values.

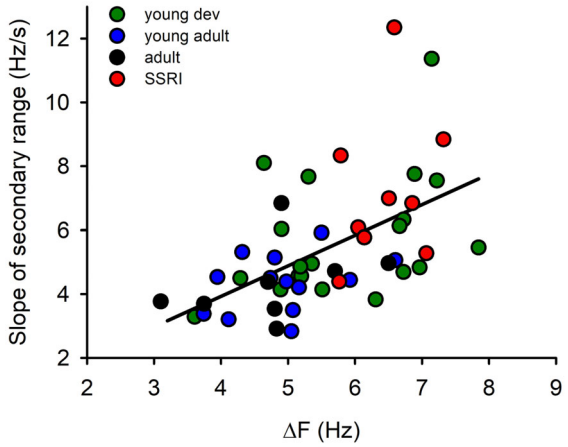

Figure 8. ΔF versus slope of secondary range
The average secondary range slope plotted against the corresponding average ΔF in each participant (n = 50): young development (green), young adult (blue), adult (black) and SSRI (red). The black regression line was fit through all data points. [Colour figure can be viewed at wileyonlinelibrary.com]

Start, maximum and end firing rates across motor unit recruitment threshold

The start, maximum and end firing rates were further analysed based on the recruitment threshold of the motor units (Fig. 11). When tested with a one-way ANOVA, there was no main effect of recruitment threshold of the motor units on the start or end firing rates in any in any of the groups (see non-bold numbers in the Supporting information, Table S9a). By contrast, a one-way ANOVA

on ranks showed a significant main effect of recruitment threshold on the maximum firing rates in the young adults (marked with an asterisk in Fig. 11; $H_{1,12} = 22.850$, $P = 0.029$), increasing as the recruitment threshold increased. When taking the recruitment threshold of the motor units into account, the higher firing rates in the young development and SSRI groups compared to the adults and age-matched controls, respectively, were more apparent. The two-way ANOVA showed a significant main effect of group on the start, maximum and end rates between the young development and young adult groups and for the maximum and end firing rates between the young development and adult groups (solid circles in Fig. 11; see also bold values in the Supporting information, Table S9b). Similarly, the two-way ANOVA showed a significant main effect of group for the start and maximum firing rates between the SSRI and SSRI control groups.

Maximum firing rate *vs.* recruitment threshold of motor unit

We further investigated the relationship between maximal firing rates and recruitment threshold of the motor units (e.g. Fig. 12*A*) by calculating the repeated measures correlation coefficients (*rmcc*) for each participant within each group. Across all groups, the relationship between the maximum firing rates and recruitment threshold of the motor units was significantly positive during contractions performed up to 30% MVC (Fig. 12*B*–*F*), indicating that the recruitment threshold and firing rate patterns did not follow an onion skin pattern as in De Luca & Hostage (2010). Although this relationship was significantly positive in all groups, it varied from very weak in the adults [$r_{533} = 0.12$ (0.037, 0.2), $P = 0.005$] to moderate in the young development [$r_{610} = 0.27$ (0.2, 0.34), $P < 0.0001$] and SSRI groups [$r_{420} = 0.28$ (0.19, 0.37), $P < 0.0001$], whereas the young adult [$r_{667} = 0.21$ (0.14, 0.28), $P < 0.0001$] and SSRI control [$r_{1133} = 0.21$ (0.15, 0.26), $P < 0.0001$] groups were in between. The stronger relationship in the young development and SSRI groups occurred because the higher threshold units (blue) typically had higher firing rates compared to the lower threshold units, as shown for the superimposed polynomial firing rate profiles in a representative SSRI participant (Fig. 12*G*). By contrast, some (but not all) of the highest threshold units in the adults had lower firing

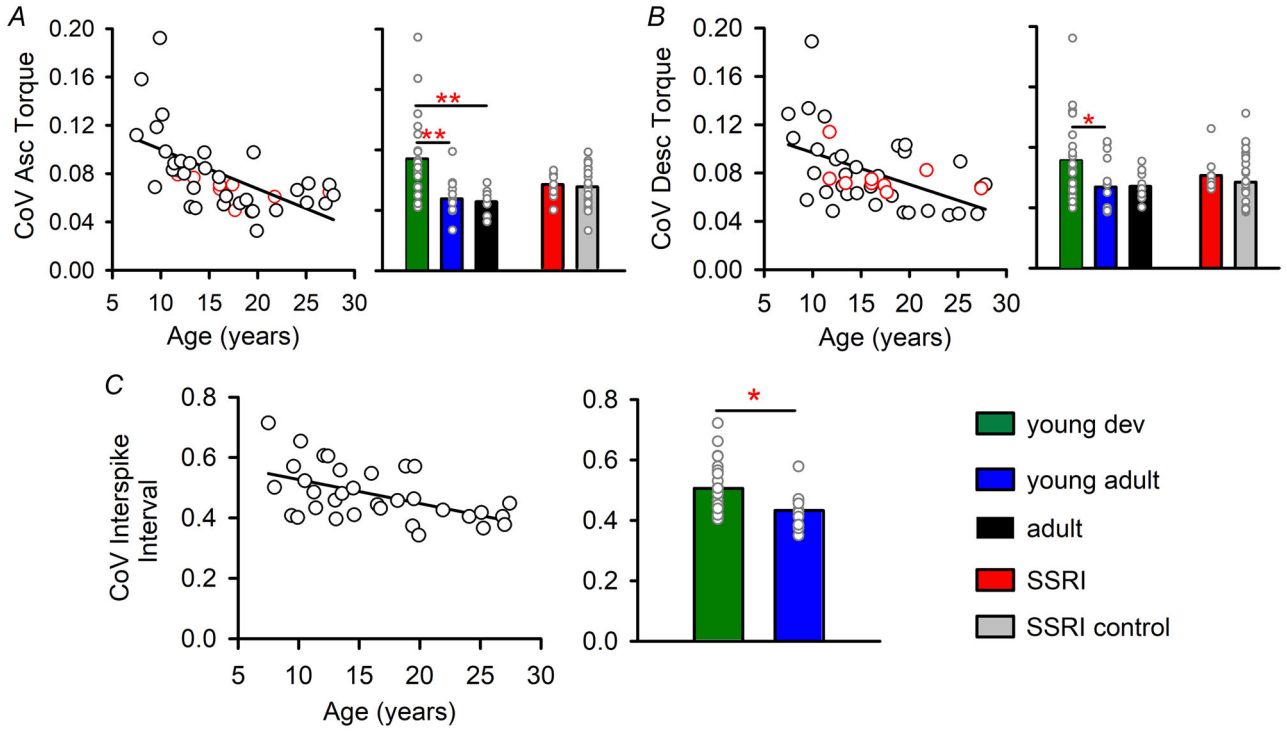

Figure 9. Variability of torque steadiness and interspike interval
Left: average coefficient of variation (CoV) of the detrended torque plotted by age across the young development and young adult groups for the ascending (*A*) and descending (*B*) phase of the contraction. The black line indicates a significant correlation. Participants taking SSRIs are marked by red open circles and were not included in the regression. Right: height of bar indicates mean value for each group with individual participant data marked by small circles. *C*, left: average CoV of the interspike interval for all motor units in each participant plotted against age for the young development and young adult groups. Right: as in (*A*) and (*B*) but for young development and young adult groups only. $*P < 0.05$ and $**P < 0.01$, denotes significant differences between groups (see bold numbers in the Supporting information, Table S7c). [Colour figure can be viewed at wileyonlinelibrary.com]

rates compared to the lowest-threshold units (Fig. 12*H*), resulting in a shallower slope and lower *rmcc*.

Discussion

In rodents, during the first 3 weeks after birth, motoneuron PICs decrease in threshold and increase in amplitude to help secure motoneuron recruitment and amplify synaptic inputs (Quinlan et al., 2011; Sharples & Miles, 2021). At early developmental stages *in vitro*, PICs produce little self-sustained activation of the motoneuron that would prolong the effects of synaptic inputs, especially in small motoneurons (Harris-Warrick et al., 2023). Using indirect methods, in the present study, we show in humans that, by 7 years of age, motoneurons have appreciable self-sustained activity, with participants

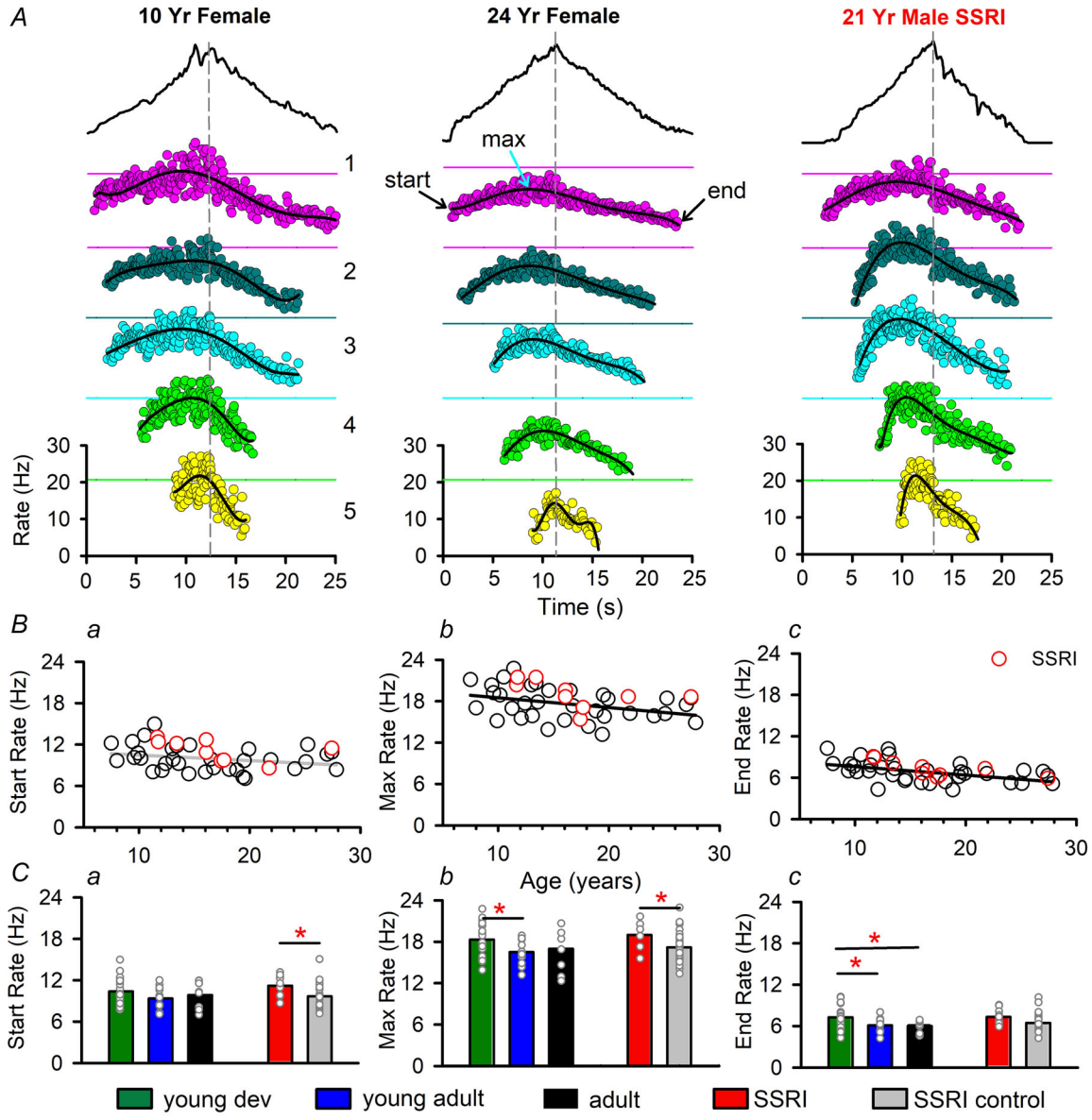

Figure 10. Start, maximum and end firing rates
A, representative firing rate profiles of motor units used to measure the start, maximum, and end firing rates from the fit fifth-order polynomial line (black). Left: 10-year-old (yr) female. Middle: 24-year-old female. Right: 24-year-old male taking an SSRI. The horizontal lines matched to the colour of the corresponding motor unit indicate the baseline of 0 Hz (except for the last yellow unit). *B*, similar format to Fig. 3 with start (*Ba*), maximum (*Bb*) and end (*Bc*) firing rates plotted against age for the young development and young adult groups. *C*, similar format to Fig. 3 for start (*Ca*), maximum (*Cb*) and end (*Cc*) firing rates. *Statistically significant difference between groups with $P < 0.05$; results of unpaired comparisons are presented in the text and Supporting information (Table S8c). [Colour figure can be viewed at wileyonlinelibrary.com]

between the ages of 7 and 17 years having larger ΔF values compared to participants between the ages of 18 to 28 years or 32 to 53 years of age. We also directly quantified the slope and duration of the initial acceleration in motor unit firing (secondary range) during a slowly increasing synaptic drive as an indirect measure of the size of the PIC effect during its initial, abrupt activation. Because PIC activation is initiated over a fixed time in an all-or-none manner (Bennett et al., 1998), faster increases in firing during the secondary range should occur for larger PICs (Afsharipour et al., 2020), as detailed further below. Furthermore, PICs are activated subthreshold to firing and continue to activate rapidly at the onset of firing, and thus, lower threshold PICs that are in the steep part of their activation at recruitment should lead to a steeper secondary range. Taken together, steeper secondary range slopes suggest larger, lower threshold PICs and is consistent with our finding that motoneurons with larger estimated PICs by the ΔF method have steeper secondary range slopes. For example, the young development group had both larger ΔF values and secondary range slopes compared to adults, suggesting the motoneurons had larger and lower threshold PICs before and during adolescence compared to adulthood. Similarly, in participants taking SSRIs, both measures of PIC activation, ΔF and the slope of the secondary range, were also larger and steeper respectively compared to their age-matched controls, consistent with serotonin increasing the amplitude and decreasing the threshold of motoneuron PICs (Harvey et al., 2006a; Li et al., 2007). The increased excitability of motoneuron PICs was also associated with higher firing rates in the young development and SSRI groups. Below, we discuss some of the intrinsic and extrinsic factors that may produce the developmental changes in motoneuron excitability that could combine to lower the torque steadiness and

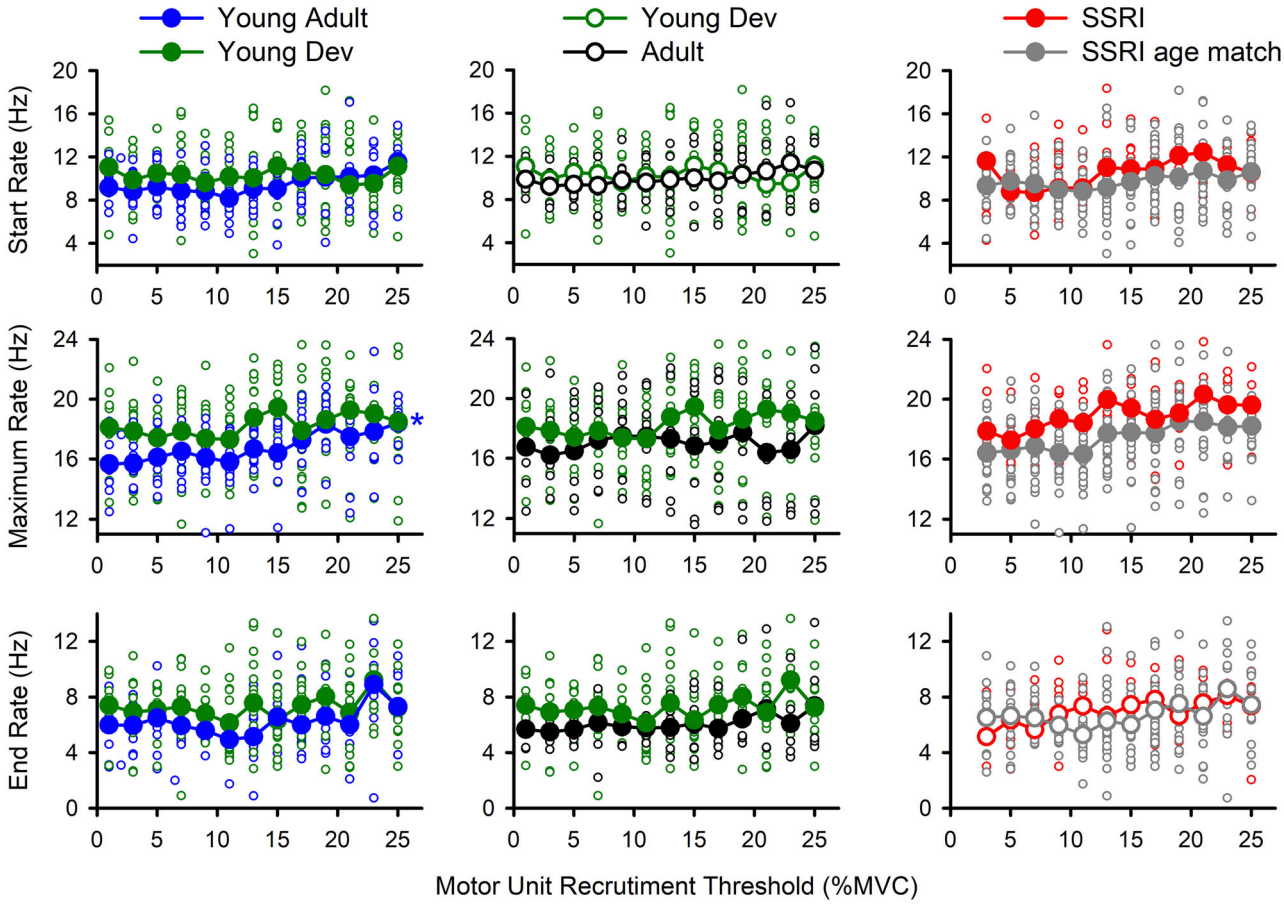

Figure 11. Start, maximum and end firing rates according to recruitment threshold of the motor units
The start (top), maximum (middle), and end (bottom) firing rates plotted against the recruitment threshold of the motor units for the young development (green), young adult (blue), adults (black), SSRI (red), and SSRI-age matched controls (grey). *Statistically significant effect of recruitment threshold on maximum firing rate in the young adult group (bold numbers for one-way ANOVA in the Supporting information, Table S9a). Solid symbols indicate significant effect of group on the start, maximum or end rate from a two-way ANOVA (bold numbers in the Supporting information, Table S9b). Small circles indicate individual participant values. [Colour figure can be viewed at wileyonlinelibrary.com]

dorsiflexion skill observed in the young development group.

Relation of the secondary range and start rates to PIC activation

The initial acceleration in firing rate at the onset of motor unit recruitment, as quantified by the slope and duration of the secondary range, is assumed to be produced by the low-voltage activation of the PIC near the onset of motoneuron recruitment (Afsharipour et al., 2020; Bennett et al., 1998; Binder et al., 2020; Lee & Heckman, 1998). In addition, a slow inactivation of Kv1.2 channels in the axon initial segment may also contribute to the firing rate acceleration during the secondary range (Bos et al., 2018). This could occur if the Kv1.2 channels were activated quickly at the onset of firing to resist recruitment and then slowly inactivated over the next few seconds to facilitate the initial firing rate acceleration mediated by the increasing synaptic input and PIC. As we have previously predicted (Afsharipour et al., 2020), motor units with low recruitment thresholds have a steeper secondary range slope compared to higher threshold units (Fig. 7). A steep secondary range in low threshold units could be produced if a substantial portion of the PIC is activated subthreshold to firing, with initial motor unit firing occurring during the latter, steep rising portion of the PIC. By contrast, the shallower secondary range slope in the higher threshold motor units could result from the PIC being activated closer to motoneuron recruitment where the initial acceleration of the PIC is slower (Bennett et al., 1998; Binder et al., 2020; Svirskis & Hounsgaard, 1997).

The finding that the young development and SSRI participants had a shorter duration secondary range

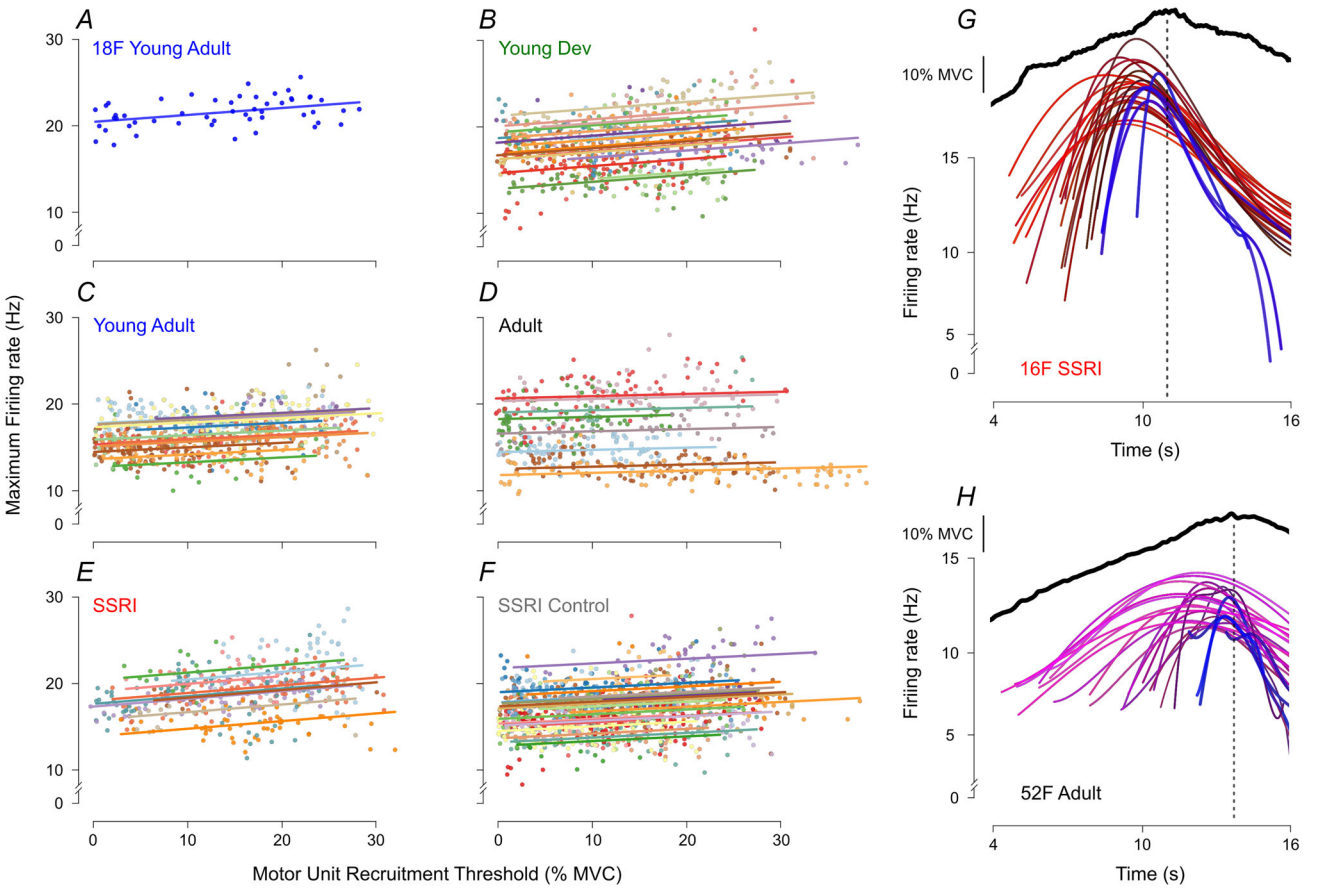

Figure 12. Relation of maximum firing rate and motor unit recruitment threshold
A, straight line fit through data points of maximum firing rate (obtained from the fit polynomial line) plotted against recruitment threshold for all motor units from four contractions in an 18-year-old female participant. *B–F*, best linear fit from the analysis of covariance for each participant using parallel regression lines but with unique *y*-intercepts for the young development (*B*), young adult (*C*), adult (*D*), SSRI (*E*) and SSRI age-matched controls (*F*). Each participant is identified with a different colour. *G*, overlay of polynomial fits to the firing rate profiles for one contraction from a 16-year-old female participant in the SSRI group, as well as from a 52-year-old female participant in the adult group (*H*). [Colour figure can be viewed at wileyonlinelibrary.com]

would also suggest that the PICs in these two groups have a reduced threshold compared to the adult groups. In support of this, one of the major effects of serotonin is to reduce the threshold of the PIC (Li et al., 2007) and this might contribute to more of the lowest threshold units in the SSRI group having a brief, or even lack of a secondary range with firing starting directly on the tertiary range (Fig. 5). Similarly, when taking recruitment threshold into account, the start rates of the motor units in the young development and SSRI groups were also higher compared to the adults and age-matched controls, consistent with larger and more rapidly activating PICs at recruitment. As discussed below (see 'Functional consequences of lower threshold and larger PICs in the young development group'), a steep secondary range and high initial firing rate produced by a large subthreshold PIC may not only provide a more secure recruitment of motor units, but also may make gradually increasing torque at the onset of a contraction more difficult if several motor units are abruptly recruited together at high firing rates (Del Vecchio, Sylos-Labini et al., 2020).

Larger SSD and/or ΔF in young development and SSRI participants

Interestingly, our results demonstrate that the slope of the secondary range may be a very effective and simpler estimate of PIC activation given that participants with steep secondary range slopes also had longer self-sustained firing as estimated by the ΔF (see correlation in Fig. 8), suggesting that the two measures could be used interchangeably even though they represent different aspects of PIC activation. The larger self-sustained firing, as measured by the ΔF, may be produced by a larger (or more sustained) motoneuron PIC in the young development and SSRI groups compared to the adults and age-matched controls, respectively. The SSD, which uses the torque profile as an estimate of the synaptic input to the motoneurons, may also reflect the contribution of the PIC to self-sustained firing but could be less sensitive because larger SSD values were only seen for the SSRI group compared to the age-matched controls. The larger self-sustained firing (ΔF) in the young development group may result, in part, from reduced spinal inhibition. Excitatory reflexes, such as the stretch reflex, show an age-related decline during childhood that reaches adult levels around 12–14 years, potentially from a maturation of inhibitory spinal circuitry (Geertsen et al., 2017; Willerslev-Olsen et al., 2014), the latter which reduces PICs (Bennett et al., 1998; Hyngstrom et al., 2007; Hyngstrom et al., 2008). Hormones, such as oestradiol and testosterone, facilitate the maturation of inhibitory GABAergic signalling (Gilfarb & Leuner, 2022). Because these hormones increase during the young development period (Barrientos et al., 2019; Wood et al., 2019), increases in the excitability of inhibitory circuitry may contribute to the age-related decrease in self-sustained firing we observed in this study. We did not measure whether participants in the young development group were before, within or after puberty, to determine whether motoneuron PICs changed in direct relation to predicted changes in sex hormones. There may also be a developmental decrease in the activation of the thermosensitive, transient receptor potential melastatin 5 (i.e. Trpm5) channel, which is the main sodium ion carrier for I_{CaN} that also contributes to the self-sustained firing of spinal motoneurons in young (postnatal days 5–12) mice (Bos et al., 2021). Lastly, the larger self-sustained firing (ΔF) in the SSRI group may result from the direct facilitation of the Na_V and Ca_V channels that mediate the PIC via activation of serotonin (i.e. 5-$HT2_{B/C}$) receptors on the motoneuron (D'Amico et al., 2013; Goodlich et al., 2023; Murray et al., 2010; Murray et al., 2011; Wei et al., 2014) or microglia (El Oussini et al., 2016).

Confounds of different motor unit numbers and thresholds between groups in measuring ΔF

The smaller number of decomposed motor units in the young development group, potentially as a result of muscles with smaller cross-sectional area (Del Vecchio, Holobar et al., 2020; Oliveira et al., 2022; Taylor et al., 2022), may have biased the sampling of test motor units with higher ΔF values compared to adults. However, when participants in the young adult and adult groups with a similar number of decomposed motor units were selected, the mean ΔF was still lower compared to the young development group. The young development and SSRI groups also had a smaller proportion of low threshold motor units, potentially because smaller action potentials that were less readily decomposed from the HDsEMG) that could have lower ΔFs. For example, measuring ΔF in the lowest threshold test units could have a floor effect where the firing rate of the composite control motor units when the test motor units are de-recruited cannot reach rates that are lower than the rate when the test motor units are recruited early in the contraction. However, there were no effects of motor unit recruitment threshold on the differences in ΔF in any of the group comparisons, in agreement with earlier studies (Afsharipour et al., 2020). Moreover, the ΔF values of the lowest threshold units activated between 0% and 3% MVC, which probably includes small slow motoneurons, were just as large as those of the higher threshold units. This contrasts with mice motoneurons recorded *in vitro* up to adolescence (3 weeks) where small motoneurons lack self-sustained (bistable) activity (Harris-Warrick et al., 2023), raising the question of whether differences in species (mice *vs.*

human) or recording conditions (*in vitro vs. in vivo*) are driving these different findings.

Estimation of input/output gain of motoneurons from the tertiary range

There appears to be a slightly higher gain in transducing firing frequency from synaptic inputs in motoneurons of the young development group compared to young adults. That is, the slope of the tertiary range when compared across motor units of different recruitment threshold was slightly larger in the young development group compared to the young adult group, although this was a weak effect not seen in the overall group averages. This would suggest that the transduction of synaptic inputs into motoneuron firing following full PIC activation occurs at a higher gain in the young development group and agrees with the overall observed higher firing rates; however, differences in synaptic inputs between groups cannot be ruled out. Further experiments with better quantifiable and controlled synaptic inputs, such as those generated during muscle stretch (Gorassini et al., 1999; Powers et al., 2008), are needed to examine the true input/output gain of the tertiary range and determine whether it varies across development (Smith & Brownstone, 2020), after brain or spinal cord injury (Harvey et al., 2006a) or from motoneuron disease such as amyotrophic lateral sclerosis (Huh et al., 2021; Jensen et al., 2020) as shown in animal models.

Direct measurement of the secondary and tertiary ranges

We have demonstrated that it is important to measure the secondary and tertiary range slopes directly using optimization techniques, which demonstrates a strong relationship between the secondary range slope and the ΔF (PIC) and subtle changes in tertiary slope that reflect motoneuron gain as detailed above. Other indirect methods of estimating these slopes were suggested (Beauchamp et al., 2023), including our work where only a single slope was fit to the ascending or descending firing rate profile (Afsharipour et al., 2020), and have produced different findings. For example, the average slope of the tertiary range using our optimization technique is $\sim$0.6 Hz s^{-1}, which was around 10 times shallower than the average slope of the secondary range at $\sim$6.0 Hz s^{-1}. These slope values are higher compared to the slopes measured by drawing a straight line from the discharge rate at motor unit recruitment to the firing rate at the end of the ascending phase of the contraction and measuring the location of the longest orthogonal line to determine the transition point between the secondary and tertiary ranges; secondary range slope: 2.44 Hz s^{-1}, tertiary range slope: 0.4 Hz s^{-1} in Beauchamp et al. (2023). The lower slopes from this method probably stem from including more of the tertiary range into the secondary range and not excluding the tertiary sag range in contrast to when these slopes are directly fitted with three joined straight lines from our linear piecewise method.

Higher motor unit firing rates in young development and SSRI participants

Previous reports have suggested that in prepubescent children, firing rates in first dorsal interosseous motor units are higher compared to adults at matched levels of MVC force to compensate for the inability to activate motor units with high recruitment thresholds (Dotan et al., 2012; Miller et al., 2019). In agreement with this and other studies (Okudaira et al., 2023; Piotrkiewicz et al., 2007), we also show that the maximum and end firing rates of TA motor units decrease with age from 7 to 28 years, with the young development group having higher firing rates compared to the young adult and/or adult groups. Although superimposition of motor unit action potentials at peak contractions may reduce the accuracy of decomposition and measures of maximum firing rates, the finding that the end firing rates were also higher, where there is less superimposition, supports the conclusion of higher maximum firing rates in the young development group. The higher firing rates in the young development group may be produced by a higher synaptic drive needed to reach a comparable level of 30% MVC torque compared to the adult groups if not as many large, fast motor units with higher force generation were recruited (Dotan et al., 2012). Alternatively, or in addition, the higher firing rates in the young development group may result from motoneurons with shorter AHPs, as demonstrated for biceps motoneurons in 5.5–19-year-old compared to 37.5–79-year-old participants (Piotrkiewicz et al., 2007). Whatever the mechanism, the need to contract against a higher antagonist (e.g., soleus) load likely did not contribute to the higher firing rates in the TA motor units. The higher firing rates in the young participants might be matched to their faster twitch contraction times, where, in the TA muscle, it progressively slows from 20 to 100 years of age (Vandervoort & McComas, 1986) and are probably even shorter at earlier ages.

Unexpectedly, the end firing rates were not lower in the young development or SSRI groups even though the PICs may have been larger compared to the adults and age-matched controls, respectively, where NaPICs could regeneratively drive very slow firing rates at low synaptic drive near de-recruitment (Li et al., 2004). Perhaps the synaptic drive at the end of the contraction decreased too rapidly to allow for appreciable NaPIC-mediated discharge that is more readily seen during a steady,

weak contraction (Gorassini et al., 2004). The start and maximum firing rates were also higher in the SSRI group compared to the age-matched controls, consistent with 5-HT increasing the input resistance of the motoneuron (Harvey et al., 2006a), facilitating the NaPIC and shortening the AHP (Harvey et al., 2006b; Perrier et al., 2013) to possibly produce higher rates of initial and steady firing.

Increasing maximum firing rates with recruitment threshold of the motor units

Different methods of isolating single motor units from EMG signals have led to different conclusions between firing rates and recruitment threshold, which we reinvestigate here. Studies utilizing intramuscular EMG and visual motor unit identification have shown that low threshold motor units peak at lower rates and forces compared to higher threshold motor units where firing rates continue to increase up to 100% MVC (Barry et al., 2007; Gydikov & Kosarov, 1974; Jesunathadas et al., 2012; Moritz et al., 2005; Oya et al., 2009). This pattern of firing rate discharge is logical for efficient muscle force production because low threshold motor units achieve peak tetanic forces at lower firing rates compared to higher threshold units given the slower twitch contraction times in the former (Piotrkiewicz & Turker, 2017). Thus, the low firing rates in lower threshold motor units keep the maximum firing rates tuned to their slower contraction times, potentially preventing unnecessary high firing rates and energy expenditure (Burke, 1968). Similarly, we also observe a positive relationship between maximum firing rates and recruitment threshold of the motor units isolated with HDsEMG and blind source decomposition where several motor units can be simultaneously identified during a single contraction. However, in some cases, the firing rates of the highest threshold motor units recruited near peak torque were less than the lower threshold motor units (e.g. dark blue profiles in Fig. 12*H*). This may be produced by a reduced availability of increasing supra-threshold current near the 30% MVC peak torque to drive the firing rates higher (Powers & Heckman, 2017). Future experiments will examine whether the firing rates of these motor units can be driven higher by larger synaptic inputs during contractions that are >30% MVC.

How are these results reconciled with other studies which show a decrease in maximum firing rates as the recruitment threshold of the motor unit increases to produce the onion skin effect? Previous studies showing an onion skin effect in the TA at comparable contraction intensities (20% to 50% MVC) were decomposed using five-pin surface arrays and a precision decomposition technique (De Luca & Hostage, 2010; Nawab et al., 2010). This technique is prone to a greater probability of missing spikes from the superimposition of motor units during stronger contraction intensities (Farina & Enoka, 2011). Thus, missed spikes in the higher threshold units at higher forces would artificially produce lower firing rates. Precision decomposition also selects motor unit activation times based on the unit's local predicted firing rate, potentially producing artificially higher firing rates in the lower threshold units as well. By contrast, motor units visually isolated from intramuscular EMG or from 64-electrode HDsEMG and blind source decomposition may be less susceptible to missed spikes and forced firing rate profiles (Caillet et al., 2023; Farina & Enoka, 2011) and thus, show higher firing rates in progressively activated motor units. Therefore, we suggest that in the TA, decreases in maximum firing rates with recruitment in the onion skin effect is an artifact of missed spikes and/or forced firing rate profiles when using 5-pin surface arrays and precision decomposition. However, further studies using HDsEMG and blind source decomposition at higher contractions are needed to determine whether increases in maximum firing rates with recruitment threshold is still maintained, as occurs with contractions up to 90% MVC for TA motor units visually identified from intramuscular EMG (Jesunathadas et al., 2012).

Functional consequences of lower threshold and larger PICs in the young development group

A lower-threshold and potentially larger motoneuron PIC in the young development group may help descending synaptic inputs recruit and prolong motoneuron firing during voluntary contractions. However, these facilitated PICs may produce a more abrupt and synchronous recruitment of motor units at higher rates of discharge, contributing to the greater firing rate variability and torque unsteadiness (i.e. higher CoV) observed during the ascending phase of the contraction in the young development group (Fig. 9). Similarly, greater self-sustained firing of motoneurons may contribute to the greater torque unsteadiness during the descending phase of the contraction, making the descending control of motoneuron de-recruitment and muscle relaxation more challenging. Although PICs are instrumental in amplifying synaptic inputs and facilitating repetitive discharge, the membrane potential of motoneurons can vary more when on a plateau potential (Bennett et al., 1998), although we do not know why this is the case. Thus, the lower threshold and larger PIC in the younger participants may introduce more variability in the motoneuron membrane potential, making the task of matching the triangular torque profile more difficult. This may be especially problematic in participants aged less than 12–14 years in whom the corticospinal tract and cortical grey matter are still undergoing substantial

anatomical and functional development (Christova & Georgopoulos, 2023; Nezu et al., 1997; Petersen et al., 2010; Yeo et al., 2014), along with a slower processing of visual information and motor execution to visual targets (Davies et al., 2015). By contrast, participants taking SSRIs also had steeper and shorter secondary ranges and more self-sustained motoneuron firing but without a larger torque unsteadiness. Because this group was older (17.02 ± 5.02 years) compared to the young development group (12.18 ± 2.69 years), the SSRI group may have a more developed visual feedforward/feedback system, corticospinal tract and spinal inhibition to help control the lower threshold and larger amplitude motoneuron PICs.

Relation to previous animal and human work and clinical implications

As mentioned in the Introduction, in rodents, the amplitude of the PIC increases in the first 3 weeks after birth as the animal gains weight bearing locomotion. We observed evidence consistent with large PIC activation producing longer self-sustained firing in motoneurons of children as young as 7 years of age where ΔF declines from 7 to 28 years and remains stable throughout adulthood (Huh et al., 2021) until it starts to decline around 65–70 years of age (Hassan et al., 2021; Orssatto et al., 2021). Given the importance of sex hormones such as oestrogens, progestogens and androgens on metabolic function in spinal motoneurons (Vegeto et al., 2020), it would be important to also look at changes in motoneuron properties according to hormonal profile across development, rather than just across chronological age. Finally, it would be interesting to determine in newborns whether motoneuron PICs, as in rodents, also start out small and non-hysteretic and become larger and more persistent to provide synaptic amplification and self-sustained firing as bipedal locomotion is achieved. None-the-less, data from this study can be used to compare to childhood neurological disorders such as cerebral palsy, Down's syndrome and spinal muscular atrophy to determine whether alterations in the threshold and persistence of PICs and transduction of synaptic inputs into firing may contribute to the motor abnormalities, such as hyper- and hypotonia, present in these conditions.

References

B., Manzur N., Duchcherer J., Fenrich K. F., Thompson C. K., Negro F., Quinlan K. A., Bennett D. J., & Gorassini M. A. (2020). Estimation of self-sustained activity produced by persistent inward currents using firing rate profiles of multiple motor units in humans. *Journal of Neurophysiology*, **124**(1), 63–85.

Bakdash J. Z., & Marusich L. R. (2017). Repeated measures correlation. *Frontiers in Psychology*, **8**, 456.

Barrientos R. M., Brunton P. J., Lenz K. M., Pyter L., & Spencer S. J. (2019). Neuroimmunology of the female brain across the lifespan: Plasticity to psychopathology. *Brain, Behavior, and Immunity*, **79**, 39–55.

Barry B. K., Pascoe M. A., Jesunathadas M., & Enoka R. M. (2007). Rate coding is compressed but variability is unaltered for motor units in a hand muscle of old adults. *Journal of Neurophysiology*, **97**(5), 3206–3218.

Beauchamp, J. A., Pearcey, G. E. P., Khurram, O. U., Chardon, M., Wang, Y. C., Powers, R. K., Dewald, J. P. A., & Heckman, C. J. (2023). A geometric approach to quantifying the neuromodulatory effects of persistent inward currents on individual motor unit discharge patterns. *Journal of Neural Engineering* **20**(1), 016034.

Bennett D. J., Hultborn H., Fedirchuk B., & Gorassini M. (1998). Synaptic activation of plateaus in hindlimb motoneurons of decerebrate cats. *Journal of Neurophysiology*, **80**(4), 2023–2037.

Bennett D. J., Li Y., Harvey P. J., & Gorassini M. (2001). Evidence for plateau potentials in tail motoneurons of awake chronic spinal rats with spasticity. *Journal of Neurophysiology*, **86**(4), 1972–1982.

Bennett D. J., Li Y., & Siu M. (2001). Plateau potentials in sacrocaudal motoneurons of chronic spinal rats, recorded in vitro. *Journal of Neurophysiology*, **86**(4), 1955–1971.

Binder, M. D., Powers, R. K., & Heckman, C. J. (2020). Nonlinear input-output functions of motoneurons. *Physiology (Bethesda, Md.)*, **35**, 31–39.

Bos R., Drouillas B., Bouhadfane M., Pecchi E., Trouplin V., Korogod S. M., & Brocard F. (2021). Trpm5 channels encode bistability of spinal motoneurons and ensure motor control of hindlimbs in mice. *Nature Communications*, **12**(1), 6815.

Bos R., Harris-Warrick R. M., Brocard C., Demianenko L. E., Manuel M., Zytnicki D., Korogod S. M., & Brocard F. (2018). Kv1.2 channels promote nonlinear spiking motoneurons for powering up locomotion. *Cell reports*, **22**(12), 3315–3327.

Bregman B. S. (1987). Development of serotonin immunoreactivity in the rat spinal cord and its plasticity after neonatal spinal cord lesions. *Brain Research*, **34**(2), 245–263.

Brix N., Ernst A., Lauridsen L. L. B., Parner E., Støvring H., Olsen J., Henriksen T. B., & Ramlau-Hansen C. H. (2019). Timing of puberty in boys and girls: A population-based study. *Paediatric and Perinatal Epidemiology*, **33**(1), 70–78.

Burke R. E. (1968). Firing patterns of gastrocnemius motor units in the decerebrate cat. *The Journal of Physiology*, **196**(3), 631–654.

Caillet A. H., Avrillon S., Kundu A., Yu T., Phillips A. T. M., Modenese L., & Farina D. (2023). Larger and denser: An optimal design for surface grids of EMG electrodes to identify greater and more representative samples of motor units. *eNeuro*, **10**(9), ENEURO.0064-23.2023.

Carrascal L., Nieto-Gonzalez J. L., Cameron W. E., Torres B., & Nunez-Abades P. A. (2005). Changes during the postnatal development in physiological and anatomical characteristics of rat motoneurons studied in vitro. *Brain Research Brain Research Reviews*, **49**(2), 377–387.

Christova P., & Georgopoulos A. P. (2023). Changes of cortical gray matter volume during development: A human connectome project study. *Journal of Neurophysiology*, **130**(1), 117–122.

D'Amico, J. M., Condliffe, E. G., Martins, K. J., Bennett, D. J., & Gorassini, M. A. (2014). Recovery of neuronal and network excitability after spinal cord injury and implications for spasticity. *Frontiers in Integrative Neuroscience*, **8**, 36.

D'amico J. M., Murray K. C., Li Y., Chan K. M., Finlay M. G., Bennett D. J., & Gorassini M. A. (2013). Constitutively active 5-HT2/α1 receptors facilitate muscle spasms after human spinal cord injury. *Journal of Neurophysiology*, **109**(6), 1473–1484.

Davies B. L., Gehringer J. E., & Kurz M. J. (2015). Age-related differences in the motor planning of a lower leg target matching task. *Human Movement Science*, **44**, 299–306.

Deluca C., & Erim Z. (1994). Common drive of motor units in regulation of muscle force. *Trends in Neuroscience (Tins)*, **17**(7), 299–305.

De Luca C. J., & Hostage E. C. (2010). Relationship between firing rate and recruitment threshold of motoneurons in voluntary isometric contractions. *Journal of Neurophysiology*, **104**(2), 1034–1046.

Del Vecchio A., Holobar A., Falla D., Felici F., Enoka R. M., & Farina D. (2020). Tutorial: Analysis of motor unit discharge characteristics from high-density surface EMG signals. *Journal of Electromyography and Kinesiology*, **53**, 102426.

Del Vecchio A., Sylos-Labini F., Mondì V., Paolillo P., Ivanenko Y., Lacquaniti F., & Farina D. (2020). Spinal motoneurons of the human newborn are highly synchronized during leg movements. *Science Advances*, **6**(47), eabc3916.

Dotan R., Mitchell C., Cohen R., Klentrou P., Gabriel D., & Falk B. (2012). Child-adult differences in muscle activation–a review. *Pediatric Exercise Science*, **24**(1), 2–21.

Dwyer, J. B., & Bloch, M. H. (2019). Antidepressants for pediatric patients. *Current Psychiatry*, **18**, 26–42F.

El Oussini H., Bayer H., Scekic-Zahirovic J., Vercruysse P., Sinniger J., Dirrig-Grosch S., Dieterlé S., Echaniz-Laguna A., Larmet Y., Müller K., Weishaupt J. H., Thal D. R., Van Rheenen W., Van Eijk K., Lawson R., Monassier L., Maroteaux L., Roumier A., Wong P. C., Van Den Berg L. H., Ludolph A. C., Veldink J. H., Witting A., & Dupuis L. (2016). Serotonin 2B receptor slows disease progression and prevents degeneration of spinal cord mononuclear phagocytes in amyotrophic lateral sclerosis. *Acta Neuropathologica*, **131**(3), 465–480.

Erim Z., De Luca C. J., Mineo K., & Aoki T. (1996). Rank-ordered regulation of motor units. *Muscle & Nerve*, **19**(5), 563–573.

Farina D., & Enoka R. M. (2011). Surface EMG decomposition requires an appropriate validation. *Journal of Neurophysiology*, **105**(2), 981–982.

Geertsen S. S., Willerslev-Olsen M., Lorentzen J., & Nielsen J. B.o (2017). Development and aging of human spinal cord circuitries. *Journal of Neurophysiology*, **118**(2), 1133–1140.

Gilfarb R. A., & Leuner B. (2022). GABA system modifications during periods of hormonal flux across the female lifespan. *Frontiers in Behavioral Neuroscience*, **16**, 802530.

Goodlich B. I., Del Vecchio A., Horan S. A., & Kavanagh J. J. (2023). Blockade of 5-HT(2) receptors suppress motor unit firing and estimates of persistent inward currents during voluntary muscle contraction in humans. *The Journal of Physiology*, **601**(6), 1121–1138.

Gorassini M., Bennett D. J., Kiehn O., Eken T., & Hultborn H. (1999). Activation patterns of hindlimb motor units in the awake rat and their relation to motoneuron intrinsic properties. *Journal of Neurophysiology*, **82**(2), 709–717.

Gorassini M., Yang J. F., Siu M., & Bennett D. J. (2002a). Intrinsic activation of human motoneurons: Possible contribution to motor unit excitation. *Journal of Neurophysiology*, **87**(4), 1850–1858.

Gorassini M., Yang J. F., Siu M., & Bennett D. J. (2002b). Intrinsic activation of human motoneurons: reduction of motor unit recruitment thresholds by repeated contractions. *Journal of Neurophysiology*, **87**(4), 1859–1866.

Gorassini M. A., Bennett D. J., & Yang J. F. (1998). Self-sustained firing of human motor units. *Neuroscience Letters*, **247**(1), 13–16.

Gorassini M. A. (2004). Role of motoneurons in the generation of muscle spasms after spinal cord injury. *Brain*, **127**(10), 2247–2258.

Granit R., Kernell D., & Lamarre Y. (1966). Synaptic stimulation superimposed on motoneurones firing in the 'secondary range' to injected current. *The Journal of Physiology*, **187**(2), 401–415.

Gydikov A., & Kosarov D. (1974). Some features of different motor units in human biceps brachii. *Pflugers Archiv: European Journal of Physiology*, **347**(1), 75–88.

Harris-Warrick, R. M., Pecchi, E., Drouillas, B., Brocard, F., & Bos, R. (2023). A size principle for bistability in mouse spinal motoneurons. *bioRxiv*. https://doi.org/10.1101/2023.09.29.559784.

Harvey P. J., Li X., Li Y., & Bennett D. J. (2006a). 5-HT2 receptor activation facilitates a persistent sodium current and repetitive firing in spinal motoneurons of rats with and without chronic spinal cord injury. *Journal of Neurophysiology*, **96**(3), 1158–1170.

Harvey P. J., Li Y., Li X., & Bennett D. J. (2006b). Persistent sodium currents and repetitive firing in motoneurons of the sacrocaudal spinal cord of adult rats. *Journal of Neurophysiology*, **96**(3), 1141–1157.

Hassan A. S., Fajardo M. E., Cummings M., Mcpherson L. M., Negro F., Dewald J. P. A., Heckman C. J., & Pearcey G. E. P. (2021). Estimates of persistent inward currents are reduced in upper limb motor units of older adults. *The Journal of Physiology*, **599**(21), 4865–4882.

Hounsgaard J., Hultborn H., Jespersen B., & Kiehn O. (1988). Bistability of alpha-motoneurones in the decerebrate cat and in the acute spinal cat after intravenous 5-hydroxytryptophan. *The Journal of Physiology*, **405**(1), 345–367.

Huh S., Heckman C. J., & Manuel M. (2021). Time course of alterations in adult spinal motoneuron properties in the SOD1(G93A) mouse model of ALS. *eNeuro*, **8**(2), ENEURO.0378-20.2021.

Hyngstrom A. S., Johnson M. D., & Heckman C. J. (2008). Summation of excitatory and inhibitory synaptic inputs by motoneurons with highly active dendrites. *Journal of Neurophysiology*, **99**(4), 1643–1652.

Hyngstrom A. S., Johnson M. D., Miller J. F., & Heckman C. J. (2007). Intrinsic electrical properties of spinal motoneurons vary with joint angle. *Nature Neuroscience*, **10**(3), 363–369.

Jean-Xavier C., Sharples S. A., Mayr K. A., Lognon A. P., & Whelan P. J. (2018). Retracing your footsteps: Developmental insights to spinal network plasticity following injury. *Journal of Neurophysiology*, **119**(2), 521–536.

Jensen D. B., Kadlecova M., Allodi I., & Meehan C. F. (2020). Spinal motoneurones are intrinsically more responsive in the adult G93A SOD1 mouse model of amyotrophic lateral sclerosis. *The Journal of Physiology*, **598**(19), 4385–4403.

Jesunathadas M., Klass M., Duchateau J., & Enoka R. M. (2012). Discharge properties of motor units during steady isometric contractions performed with the dorsiflexor muscles. *Journal of Applied Physiology (1985)*, **112**(11), 1897–1905.

Kernell D. (1965). High-frequency repetitive firing of cat lumbosacral motoneurones stimulated by long-lasting injected currents. *Acta Physiologica Scandinavica*, **65**(1–2), 74–86.

Kiehn O., & Eken T. (1997). Prolonged firing in motor units: Evidence of plateau potentials in human motoneurons? *Journal of Neurophysiology*, **78**(6), 3061–3068.

Lee R. H., & Heckman C. J. (1998). Bistability in spinal motoneurons in vivo: Systematic variations in persistent inward currents. *Journal of Neurophysiology*, **80**(2), 583–593.

Lee R. H., & Heckman C. J. (2000). Adjustable amplification of synaptic input in the dendrites of spinal motoneurons in vivo. *Journal of Neuroscience*, **20**(17), 6734–6740.

Lee R. H., Kuo J. J., Jiang M. C., & Heckman C. J. (2003). Influence of active dendritic currents on input-output processing in spinal motoneurons in vivo. *Journal of Neurophysiology*, **89**(1), 27–39.

Li X., Murray K., Harvey P. J., Ballou E. W., & Bennett D. J. (2007). Serotonin facilitates a persistent calcium current in motoneurons of rats with and without chronic spinal cord injury. *Journal of Neurophysiology*, **97**(2), 1236–1246.

Li Y., Gorassini M. A., & Bennett D. J. (2004). Role of persistent sodium and calcium currents in motoneuron firing and spasticity in chronic spinal rats. *Journal of Neurophysiology*, **91**(2), 767–783.

Mcneil C. J., Doherty T. J., Stashuk D. W., & Rice C. L. (2005). Motor unit number estimates in the tibialis anterior muscle of young, old, and very old men. *Muscle & Nerve*, **31**(4), 461–467.

Miller J. D., Sterczala A. J., Trevino M. A., Wray M. E., Dimmick H. L., & Herda T. J. (2019). Motor unit action potential amplitudes and firing rates during repetitive muscle actions of the first dorsal interosseous in children and adults. *European Journal of Applied Physiology*, **119**(4), 1007–1018.

Mizuno N., & Itoh H. (2009). Functions and regulatory mechanisms of Gq-signaling pathways. *Neuro-Signals*, **17**(1), 42–54.

Moritz C. T., Barry B. K., Pascoe M. A., & Enoka R. M. (2005). Discharge rate variability influences the variation in force fluctuations across the working range of a hand muscle. *Journal of Neurophysiology*, **93**(5), 2449–2459.

Murray K. C., Nakae A., Stephens M. J., Rank M., D'amico J., Harvey P. J., Li X., Harris R. L. W., Ballou E. W., Anelli R., Heckman C. J., Mashimo T., Vavrek R., Sanelli L., Gorassini M. A., Bennett D. J., & Fouad K. (2010). Recovery of motoneuron and locomotor function after spinal cord injury depends on constitutive activity in 5-HT2C receptors. *Nature Medicine*, **16**(6), 694–700.

Murray K. C., Stephens M. J., Ballou E. W., Heckman C. J., & Bennett D. J. (2011). Motoneuron excitability and muscle spasms are regulated by 5-HT2B and 5-HT2C receptor activity. *Journal of Neurophysiology*, **105**(2), 731–748.

Nawab S. H., Chang S.-S., & De Luca C. J. (2010). High-yield decomposition of surface EMG signals. *Clinical Neurophysiology*, **121**(10), 1602–1615.

Negro F., Muceli S., Castronovo A. M., Holobar A., & Farina D. (2016). Multi-channel intramuscular and surface EMG decomposition by convolutive blind source separation. *Journal of Neural Engineering*, **13**(2), 026027.

Nezua A., Kimura S., Uehara S., Kobayashia T., Tanaka M., & Saito K. (1997). Magnetic stimulation of motor cortex in children: Maturity of corticospinal pathway and problem of clinical application. *Brain & Development*, **19**(3), 176–180.

Okudaira M., Takeda R., Hirono T., Nishikawa T., Kunugi S., & Watanabe K. (2023). Motor unit firing properties during force contrl task and associations with neurological tests in children. *Pediatric Exercise Science*, **36**(1), 23–29.

Oliveira D. S. D.e, Casolo A., Balshaw T. G., Maeo S., Lanza M. B., Martin N. R. W., Maffulli N., Kinfe T. M., Eskofier B. M., Folland J. P., Farina D., & Del Vecchio A. (2022). Neural decoding from surface high-density EMG signals: Influence of anatomy and synchronization on the number of identified motor units. *Journal of Neural Engineering*, **19**(4), 046029.

Orssatto L. B. R., Mesquita R. N. O., & Phillips K. M. (2021). Looking at the bigger PICture: Understanding and counteracting the decline of persistent inward currents in older adults. *The Journal of Physiology*, **599**(23), 5137–5139.

Oya T., Riek S., & Cresswell A. G. (2009). Recruitment and rate coding organisation for soleus motor units across entire range of voluntary isometric plantar flexions. *The Journal of Physiology*, **587**(19), 4737–4748.

Perrier J.-F., Rasmussen H., Christensen R., & Petersen A. (2013). Modulation of the intrinsic properties of motoneurons by serotonin. *Current Pharmaceutical Design*, **19**(24), 4371–4384.

Petersen T. H., Kliim-Due M., Farmer S. F., & Nielsen J. B.o (2010). Childhood development of common drive to a human leg muscle during ankle dorsiflexion and gait. *The Journal of Physiology*, **588**(22), 4387–4400.

Piotrkiewicz M., Kudina L., Mierzejewska J., Jakubiec M., & Hausmanowa-Petrusewicz I. (2007). Age-related change in duration of afterhyperpolarization of human motoneurones. *The Journal of Physiology*, **585**(2), 483–490.

Piotrkiewicz M., & Türker K. S. (2017). Onion skin or common drive? *Frontiers in Cellular Neuroscience*, **11**, 2.

Powers R. K., & Heckman C. J. (2017). Synaptic control of the shape of the motoneuron pool input-output function. *Journal of Neurophysiology*, **117**(3), 1171–1184.

Powers R. K., Nardelli P., & Cope T. C. (2008). Estimation of the contribution of intrinsic currents to motoneuron firing based on paired motoneuron discharge records in the decerebrate cat. *Journal of Neurophysiology*, **100**(1), 292–303.

Quinlan K. A., Schuster J. E., Fu R., Siddique T., & Heckman C. J. (2011). Altered postnatal maturation of electrical properties in spinal motoneurons in a mouse model of amyotrophic lateral sclerosis. *The Journal of Physiology*, **589**(9), 2245–2260.

Revill A. L., Chu N. Y., Ma L.i, Leblancq M. J., Dickson C. T., & Funk G. D. (2019). Postnatal development of persistent inward currents in rat XII motoneurons and their modulation by serotonin, muscarine and noradrenaline. *The Journal of Physiology*, **597**(12), 3183–3201.

Sharples S. A., & Miles G. B. (2021). Maturation of persistent and hyperpolarization-activated inward currents shapes the differential activation of motoneuron subtypes during postnatal development. *Elife*, **10**, e71385.

Skinner J. W., Christou E. A., & Hass C. J. (2019). Lower extremity muscle strength and force variability in persons with Parkinson disease. *Journal of Neurologic Physical Therapy*, **43**(1), 56–62.

Smith C. C., & Brownstone R. M. (2020). Spinal motoneuron firing properties mature from rostral to caudal during post-natal development of the mouse. *The Journal of Physiology*, **598**(23), 5467–5485.

Svirskis G., & Hounsgaard J. (1997). Depolarization-induced facilitation of a plateau-generating current in ventral horn neurons in the turtle spinal cord. *Journal of Neurophysiology*, **78**(3), 1740–1742.

Taylor C. A., Kopicko B. H., Negro F., & Thompson C. K. (2022). Sex differences in the detection of motor unit action potentials identified using high-density surface electromyography. *Journal of Electromyography and Kinesiology*, **65**, 102675.

Thompson C. K., & Hornby T. G. (2013). Divergent modulation of clinical measures of volitional and reflexive motor behaviors following serotonergic medications in human incomplete spinal cord injury. *Journal of Neurotrauma*, **30**(6), 498–502.

Vandervoort A. A., & Mccomas A. J. (1986). Contractile changes in opposing muscles of the human ankle joint with aging. *Journal of applied physiology (1985)*, **61**(1), 361–367.

Vegeto E., Villa A., Della Torre S., Crippa V., Rusmini P., Cristofani R., Galbiati M., Maggi A., & Poletti A. (2020). The role of sex and sex hormones in neurodegenerative diseases. *Endocrine Reviews*, **41**(2), 273–319.

Wei K., Glaser J. I., Deng L., Thompson C. K., Stevenson I. H., Wang Q., Hornby T. G., Heckman C. J., & Kording K. P. (2014). Serotonin affects movement gain control in the spinal cord. *Journal of Neuroscience*, **34**(38), 12690–12700.

Willerslev-Olsen M., Andersen J. B., Sinkjaer T., & Nielsen J. B.o (2014). Sensory feedback to ankle plantar flexors is not exaggerated during gait in spastic hemiplegic children with cerebral palsy. *Journal of Neurophysiology*, **111**(4), 746–754.

Wood C. L., Lane L. C., & Cheetham T. (2019). Puberty: Normal physiology (brief overview). *Best Practice & Research-Clinical Endocrinology & Metabolism*, **33**(3), 101265.

Xia Y., Chen D., Xia H., Liao Z., Tang W., & Yan Y.i (2017). Serotonergic projections to lumbar levels and its plasticity following spinal cord injury. *Neuroscience Letters*, **649**, 70–77.

Yeo S. S., Jang S. H.o, & Son S.u M. (2014). The different maturation of the corticospinal tract and corticoreticular pathway in normal brain development: Diffusion tensor imaging study. *Frontiers in Human Neuroscience*, **8**, 573.

Additional information

Data availability statement

The data that support the findings of this study are available from the corresponding author upon reasonable request. The statistical results are summarized in the Supporting information.

Competing interests

The authors declare they have no competing interests.

Author contributions

G.M., B.A., A.Y., F.N., K.A., DJB and MAG conceived and designed research. G.M., B.A., A.Y., J.D. and MAG performed experiments. G.M., B.A., A.Y., J.D., J.B., E.B., GEP and MAG analysed the data. G.M., B.A., Y.A., GEP, K.A., DJB and MAG interpreted the results of experiments. G.M., J.N., A.Y., GEP and MAG prepared figures. G.M., GEP and MAG drafted and revised the manuscript and all authors edited the manuscript. All authors approved the final version of the manuscriupt submitted for pub;ication. All authors agree to be accountable for all aspects of the work. The authors confirm that all persons designated as authors are qualified.

Funding

This work was supported by a Natural Sciences and Engineering Research Council of Canada Grant 0 5205 to MAG, an NIH RO1 NS104436 grant to KAQ and MAG, a Canadian Institute of Health Research Grant PS 180 430 to MAG, and a Women and Children's Health Research Grant 3475 to MAG.

Acknowledgements

We thank Dr Kelvin Jones for helping with the first draft of the manuscript and for advice on statistics.

Keywords

motor units, onion skin, persistent inward currents, serotonin, tibialis anterior, torque steadiness

Supporting information

Additional supporting information can be found online in the Supporting Information section at the end of the HTML view of the article. Supporting information files available:

Peer Review History
Supplemental Tables 1–10